



Fisheries and Oceans
Canada

Pêches et Océans
Canada

Ecosystems and
Oceans Science

Sciences des écosystèmes
et des océans

Canadian Science Advisory Secretariat (CSAS)

Research Document 2023/046

Quebec Region

Environmental Factors and Behaviour of St. Lawrence Estuary Beluga Generate Heterogeneity in Availability Bias for Photographic and Visual Aerial Surveys

Véronique Lesage¹, Sara Wing^{1,2}, Alain F. Zuur³, Jean-François Gosselin¹, Arnaud Mosnier¹, Anne P. St-Pierre¹, Robert Michaud⁴, Dominique Berteaux²

¹Maurice Lamontagne Institute,
Fisheries and Oceans Canada
850 Route de la Mer, Mont-Joli, Québec G5H 3Z4

²Geography, Chemistry and Biology Department,
Université du Québec à Rimouski
300 Allée des Ursulines, Rimouski, Québec, G5L 3A1

³Highlands Statistics
9 St. Clair Wynd, Newburg, AB41 6DZ, UK

⁴Groupe de recherche et d'éducation sur les mammifères marins
108 de la Cale Sèche, Tadoussac, Québec, G0T 2A0

Foreword

This series documents the scientific basis for the evaluation of aquatic resources and ecosystems in Canada. As such, it addresses the issues of the day in the time frames required and the documents it contains are not intended as definitive statements on the subjects addressed but rather as progress reports on ongoing investigations.

Published by:

Fisheries and Oceans Canada
Canadian Science Advisory Secretariat
200 Kent Street
Ottawa ON K1A 0E6

[http://www.dfo-mpo.gc.ca/csas-sccs/
csas-sccs@dfo-mpo.gc.ca](http://www.dfo-mpo.gc.ca/csas-sccs/csas-sccs@dfo-mpo.gc.ca)



© His Majesty the King in Right of Canada, as represented by the Minister of the
Department of Fisheries and Oceans, 2024

ISSN 1919-5044

ISBN 978-0-660-70322-0 Cat. No. Fs70-5/2023-046E-PDF

Correct citation for this publication:

Lesage, V., Wing, S., Zuur, A.F., Gosselin, J.-F., Mosnier, A., St-Pierre, A.P., Michaud, R., and Berteaux, D. 2024. Environmental Factors and Behaviour of St. Lawrence Estuary Beluga Generate Heterogeneity in Availability Bias for Photographic and Visual Aerial Surveys. DFO Can. Sci. Advis. Sec. Res. Doc. 2023/046. iv + 40 p.

Aussi disponible en français :

Lesage, V., Wing, S., Zuur, A.F., Gosselin, J.-F., Mosnier, A., St-Pierre, A.P., Michaud, R., et Berteaux, D. 2024. Des facteurs environnementaux et le comportement des bélugas de l'estuaire du Saint-Laurent génèrent de l'hétérogénéité dans les biais de disponibilités associés aux inventaires aériens photographiques et visuels. Secr. can. des avis sci. du MPO. Doc. de rech. 2023/046. iv + 48 p.

TABLE OF CONTENTS

ABSTRACT	iv
INTRODUCTION	1
MATERIALS AND METHODS	2
SURVEY METHODS AND STUDY AREA	2
DATA COLLECTION	4
DIVE DATA ANALYSIS	5
CORRECTING FOR AVAILABILITY BIAS	6
STATISTICAL ANALYSIS	7
CORRECTING AVAILABILITY BIAS FOR PHOTO OVERLAP	9
ESTIMATING GROUP SIZE AND ABUNDANCE	10
SENSITIVITY ANALYSIS	10
RESULTS	10
DIVE TIME	11
SURFACE TIME	11
INSTANTANEOUS AVAILABILITY (<i>P</i>)	11
MODEL SELECTION	12
SENSITIVITY ANALYSIS	13
DISCUSSION	18
ACKNOWLEDGEMENTS	23
REFERENCES CITED	23
APPENDIX 1. TURBIDITY GRADIENT IN THE ST. LAWRENCE ESTUARY	28
APPENDIX 2. EFFECTS OF DIPS BELOW TURBIDITY THRESHOLD DURING SURFACE INTERVALS ON AVAILABILITY TO VISUAL SURVEYS	29
APPENDIX 3. PROBABILITY OF A BELUGA BEING CAPTURED IN AT LEAST ONE OF TWO CONSECUTIVE PHOTOGRAPHS AS A FUNCTION OF TIME LAPSE BETWEEN FRAMES, ESTIMATED FROM TAG DATA	31
APPENDIX 4. MEAN DIVE, SURFACE TIMES AND AVAILABILITY FOR PHOTOGRAPHIC AND VISUAL SURVEYS	32
APPENDIX 5. DIVE TIME (<i>D</i>): ESTIMATED REGRESSION PARAMETERS FOR A GAMMA GAMM APPLIED TO <i>D</i>	33
APPENDIX 6. SURFACE TIME (<i>S</i>): ESTIMATED REGRESSION PARAMETERS FOR A GAMMA GAMM APPLIED TO <i>S</i>	36
APPENDIX 7. PROPORTION OF TIME AT SURFACE (<i>P</i>): ESTIMATED REGRESSION PARAMETERS FOR A BETA GAMM APPLIED TO <i>P</i>	38
APPENDIX 8. DEVIANCE EXPLAINED BY THE DIFFERENT MODELS	40

ABSTRACT

In absence of adequate data, abundance estimates for St. Lawrence Estuary (SLE) beluga obtained from visual surveys have been corrected for availability bias using factors developed for photographic surveys. Not accounting for the longer detection time associated with visual surveys will lead to an overestimation of beluga abundance relative to indices obtained from photographic surveys. This study offers a comprehensive analysis of the relative influence of multiple methodological, environmental and behavioural factors on availability bias estimates for both photographic and visual surveys using detailed dive profiles from 27 SLE beluga.

As expected, availability estimates were systematically higher for visual surveys than for photographic surveys for which time-in-view is instantaneous. However, for photographic surveys the change in methodology for estimating availability from an approach based on group visibility to one where the detailed diving patterns of individuals were logged, led to a 26—42% decrease in mean availability estimates. Our results confirmed that dives are longer when animals are inside compared to outside areas of high density (AHD), consistent with the prediction that these areas are used for behaviour like foraging. They also indicate that while some of the behavioural or environmental factors such as latent processes associated with the zone used may have a notable effect on availability, survey design (photographic or visual), characteristics of survey platforms, and observer searching patterns may be the most influential factors on availability bias. We conclude that previous estimates of SLE beluga abundance from photographic surveys were likely biased downward by an overestimation of beluga availability, and by not considering the uneven distribution of beluga among different zones with specific but undefined underlying processes.

INTRODUCTION

Abundance estimates need to be accurate to assess population conservation status, and they need to be precise to minimize the time required to detect significant population trends (Taylor et al. 2007). Survey-derived abundance estimates can be biased when the animals which are available to be counted are missed by observers (perception bias), or when they are unavailable to be counted (availability bias; Marsh and Sinclair 1989; Buckland et al. 2004; Thomas et al. 2010). These two biases vary with survey methods, potentially preventing direct comparisons between counts. The perception bias is usually at low levels for photographic surveys, and can be estimated using multiple imagery reading (Gosselin et al. 2014; Stenson et al. 2014). For visual surveys, perception bias is usually larger and can be corrected for by using a double platform survey design and applying a mark-recapture distance-sampling procedure to the data (Laake and Borchers 2004). In contrast, the availability bias is lower for visual surveys given the longer detection time they provide compared to the snapshot of potentially detectable individuals offered by photographic surveys (McLaren 1961; Laake et al. 1997; Forcada et al. 2004; Gómez de Segura et al. 2006).

The availability of individuals to be counted can be affected by several factors other than detection time, that are inherent to the species or their environment (e.g., Brown et al. 2022). In aquatic species, turbidity can limit the depth at which animals can be detected, whereas bottom depth can modulate availability by influencing diving depth and duration (e.g., Costa and Gales 2003; Pollock et al. 2006). Bottom depth effects on availability might be particularly strong in areas where feeding occurs at deeper depth (Martin and Smith 1999; Doniol-Valcroze et al. 2011). Conversely, the influence of bottom depth might be less when animals are travelling, resting, or socializing near the surface (e.g., Whitehead and Weilgart 1991). The physiological condition and reproductive status of individuals can also affect their availability. For instance, females accompanied by a calf may dive less than non-calving females or other age- or sex-classes (e.g., Dombroski et al. 2021; Brown et al. 2022). Diving capacity increases allometrically with size, causing differences in availability among age-classes, and between males and females in sexually dimorphic species (Schreer and Kovacs 1997). Juveniles or animals in lesser body condition may also forage at different depths or in different areas than adults or animals in better shape (i.e., Orgeret et al. 2019).

Beluga (*Delphinapterus leucas*) in the St. Lawrence Estuary (SLE) have been monitored for population size and trends since 1988 using aerial and systematic photographic surveys that cover their entire summer range (Kingsley and Hammill 1991; Kingsley 1998; Kingsley 2002; Gosselin et al. 2014; Mosnier et al. 2015). Surveys of this population were exclusively photographic until 2001, when regular visual line-transect surveys were initiated (Gosselin et al. 2007; 2017). Currently, all survey counts are corrected for availability bias using a correction factor developed for photographic surveys (Kingsley and Gauthier, 2002; Gosselin et al. 2017). Recognizing the lack of a proper correction factor for availability during visual surveys, the two time series have so far been treated separately, and only photographic abundance estimates have been used to model population size and trends (e.g., Mosnier et al. 2015).

The beluga (*Delphinapterus leucas*) is a particularly challenging species to survey given its highly social and gregarious nature (Michaud 2005). As a result of their clumped distribution, abundance estimates are often associated with coefficients of variation of 25–40% (e.g., Gosselin et al. 2017; Higdon and Ferguson 2017; Lowry et al. 2019). Multiple surveys conducted days apart in the SLE indicate that abundance estimation can vary by 100% in a day, even at high survey coverage (Gosselin et al. 2007; 2017).

In this study, detailed dive profiles obtained from 27 SLE beluga were used to assess availability for photographic and visual surveys. Environmental factors such as turbidity and bottom depth, and beluga behaviour were also considered for their potential improvement to availability bias corrections for the two types of surveys. Previously-identified areas of consistent aggregation were used as a proxy for higher occurrence of foraging behaviour, assuming the rest of the SLE beluga distribution range is used predominantly for transit (Lemieux-Lefebvre et al. 2012; Mosnier et al. 2016; Ouellet et al. 2021). It was postulated that abundance estimates would increase in accuracy by considering the expected behaviour and environmental conditions at each sighting's location; indirectly, this correction might increase the precision of estimates and power to detect population trends by reducing variability among replicate surveys in a given year.

MATERIALS AND METHODS

SURVEY METHODS AND STUDY AREA

Abundance estimates for SLE beluga are obtained during summer, when their distribution is the most constrained (Mosnier et al. 2010; Gosselin et al. 2017). Surveys of the SLE use systematic parallel lines with a random start placement, and line spacing of 2 nautical miles for photographic surveys, and 4 nautical miles for visual surveys (i.e., one line out of two is flown) (Figure 1; Gosselin et al. 2014). The narrow Saguenay Fjord is flown up and down on a single track, and the number of non-duplicate sightings between passes based on beluga maximum swimming speed is used as a total count (Gosselin et al. 2017).

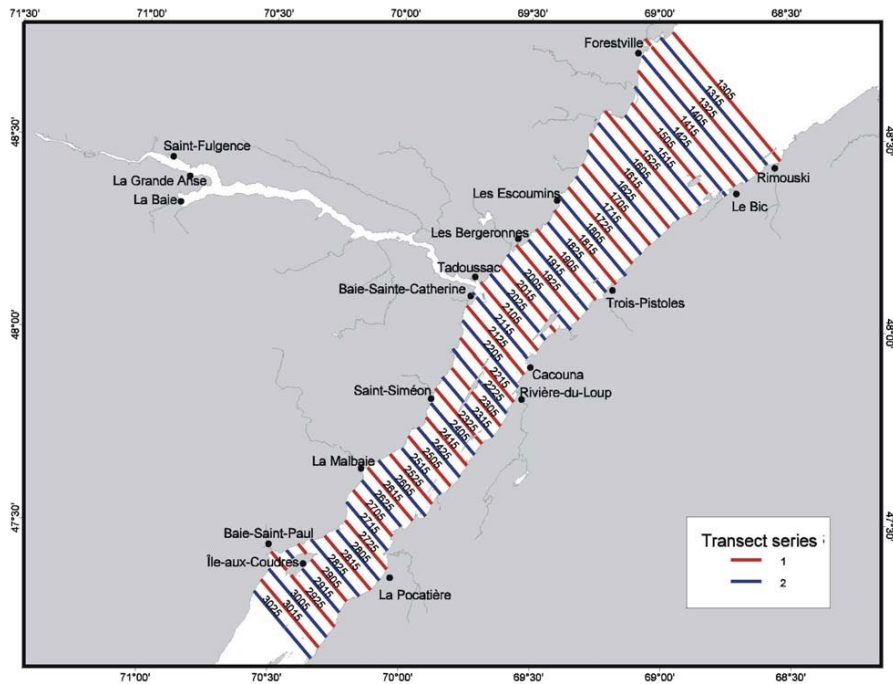


Figure 1. Survey design for SLE beluga photographic and visual surveys (the Saguenay Fjord track up to Saint-Fulgence is not shown). All lines are flown during photographic surveys, whereas only one of the two transect series is flown during visual surveys, resulting in line-spacing of 2 and 4 nautical miles, respectively (Gosselin et al. 2007).

The SLE beluga summer habitat is highly heterogeneous in bottom topography and turbidity (Figure 2; see also Supplement 1). For example, the Saguenay Fjord mouth is a few tens of

meters deep while 20 km north-east, the Laurentian Channel reaches more than 350 m. Turbidity is on average 4 m during years with no excessive rainwater runoffs, but varies between sectors from 1.5 m to 11.6 m (Kingsley and Gauthier 2002). This variability was accounted for by dividing the beluga summer habitat into three zones as per Gauthier (1999): 1) high turbidity (1.5–2.5 m) in the upstream portion of the SLE (Upper Estuary), 2) intermediate turbidity (3.5–6.5 m) in the southern half of the downstream portion of the SLE (Lower Estuary), and 3) low turbidity (4.5–11.5 m) in the northern half of the Lower Estuary (Figure 2). On the premises that white (adult) beluga are detectable at depths equivalent to Secchi-disk measurements (Kingsley and Gauthier 2002), mid-range turbidity for the three zones (i.e., 2, 5 and 8 m, respectively) were used as threshold for beluga detection.

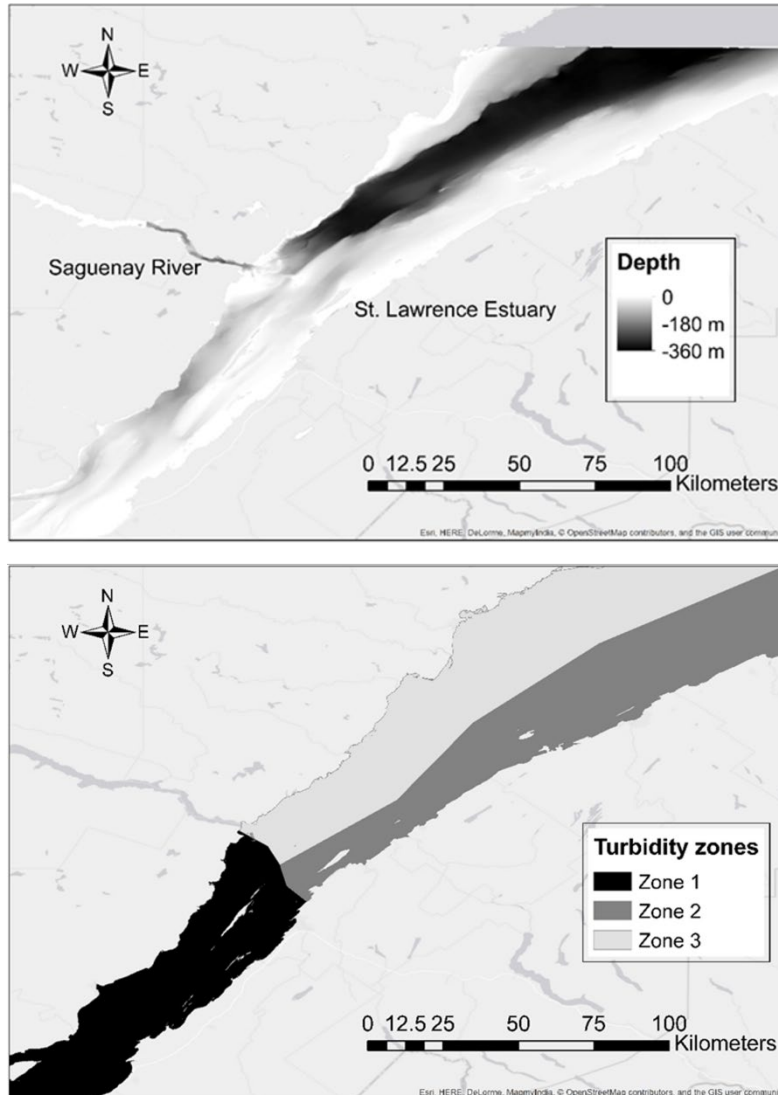


Figure 2. Seafloor depth (top panel) and turbidity zones (lower panel) in the summer range of St. Lawrence Estuary beluga (modified from Canadian Hydrographic Service, and Gauthier 1999). Turbidity, estimated using a Secchi disk, increased from zone 1 to zone 3, with mid-range turbidity values of 2 m, 5 m and 8 m, respectively (Kingsley and Gauthier 2002).

DATA COLLECTION

Effects of behaviour and environmental features on availability were examined using detailed beluga dive profiles. Tagging efforts spanned from June to September 2001–2005, over approximately 120 km in the core of the SLE beluga summer range (Figure 3), covering a variety of habitat (Mosnier et al. 2016) used by all segments of the population (Michaud 1993; Ouellet et al. 2021). A total of 44 beluga were equipped with archival tags (Time-Depth-Velocity recorders Mk8, Wildlife Computers Ltd, Redmond, WA) during this period. The instruments logged time, depth (± 0.25 m) and swim speed every second. Tags were attached with suction cups, and housed in a floating package containing a 30 g radio transmitter (VHF, Telonics, Mesa, AZ), allowing remote tracking (400–600 m) with minimal effects on behaviour (Blane and Jaakson 1994). The release system consisted of a magnesium cap machined to corrode after 4–6 h, allowing penetration of air and water under cups, and the release of suction. Tracking ceased either at dusk, when signal was lost, or when the tags came off. Some of the tags did not fall off until the following day; on these occasions, data on nighttime diving activity (but not location) were also recorded. The tracked individuals were geolocated during each surface interval using the animal's relative distance (estimated by eye or range finder) and angle from the tracking vessel (using binoculars with compass). The vessel GPS position was logged every minute. Positions for surface intervals with missing values were interpolated from the preceding and following surface interval when within 25 min from each other. This time corresponds approximately to SLE beluga maximum dive time based on tag data (Lemieux Lefebvre et al. 2018; V. Lesage, unpublished data).

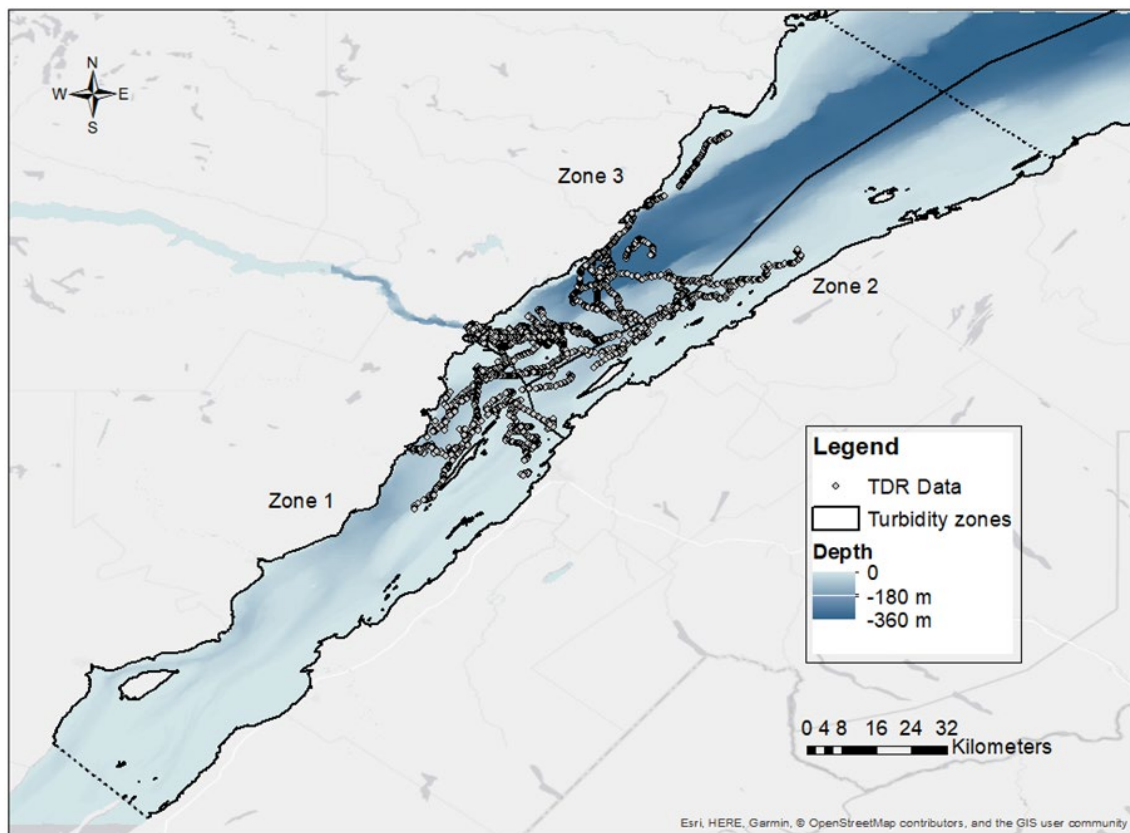


Figure 3. Spatial distribution of 27 of the 44 SLE beluga equipped with TDRs, radio-tracked from June to September 2001–2005, and retained for analyses. The black contours define the three turbidity zones (see also Figure 2). Dotted lines represent the limits of the population summer range (Michaud 1993; Gosselin et al. 2017).

DIVE DATA ANALYSIS

A custom-made program was used to obtain dive profiles and various statistics, including dive duration, time spent at the surface (post-dive) and maximum dive depth. Zero-offset correction was performed manually using Instrument Helper (Wildlife Computers Inc., Redmond, WA). The first and last intervals were removed as they were incomplete. Dive data were excluded when contact with the animal was lost for more than 25 min, during periods outside survey hours (i.e., between dusk and dawn, which varied throughout the summer), or when the tracked individual was in the Saguenay Fjord where counts are uncorrected for availability bias (Gosselin et al. 2017).

A dive was initially defined as any excursion below 0.5 m to capture series of short and shallow dives associated with surface intervals. Dive duration corresponded to the time elapsed between two successive surface intervals. A bout-ending criterion with the maximum likelihood estimation method (MLM) was used to discriminate between dives and surface intervals (Langton et al. 1995; Luque and Guinet 2007). An optimization algorithm (an extension of limited memory Broyden-Fletcher-Goldfarb-Shanno, or L-BFGS-B) was applied as part of the function to identify bouts. The upper and lower bound values were specified following Luque (2007).

During surface intervals, beluga might dip momentarily (0.1—3.6 s on average; Supplement 2) below the turbidity threshold, becoming invisible to the observer. To estimate time spent below defined turbidity thresholds and effects on availability, dive profiles were re-processed a second time: instead of using 0.5 m to define a dive, we used in turn 1) the mean turbidity threshold for the SLE beluga summer habitat (i.e., 4 m), and 2) each of the three zone-specific turbidity threshold (i.e., 2, 5 and 8 m) defined by Kingsley and Gauthier (2002). The bout-ending criterion and time stamps for surface intervals previously established using 0.5 m were used to trace back each surface interval, and identify short excursions below defined turbidity thresholds within this time frame. Results indicate that effects on availability were trivial even in the most turbid waters, with time-in-view remaining above dip time at virtually all perpendicular distances (Supplement 2). Consequently, dip time was included as part of surface time for visual surveys, and as part of dive time for photographic surveys given that the latter are based on instantaneous detections.

Areas of consistent aggregation for SLE beluga have been identified using two vast databases and different statistical approaches, which provided similar results (Lemieux Lefebvre et al. 2012; Mosnier et al. 2016). Areas of high density (AHD; 50% kernel density) obtained by Mosnier et al. (2016) from aerial survey data were retained for this analysis as they offered a full coverage of the SLE beluga summer range; whereas Lemieux-Lefebvre et al. (2012) covered only the core of their summer distribution (Figure 4). Based on the reasonable assumption that foraging most often occurs in areas of consistent aggregation, with transit occurring more frequently outside these areas, availability to a passing aircraft was postulated to be less in AHD compared to transit areas (i.e., outside of AHDs). This would be true especially if beluga feed at depth and/or tend to remain closer to the surface when transiting. Availability may also decrease with increasing seafloor depth if beluga dive to the bottom, although availability in this case would also depend on recovery time at the surface. To examine the influence of these two factors on availability, information on seafloor depth (50 m horizontal resolution; Canadian Hydrographic Service) and beluga geolocation relative to areas of consistent aggregation (inside or outside AHD) were extracted for each dive and corresponding post-dive surface interval. Each observation was also assigned to one of three turbidity zones based on geolocation (Figure 2).

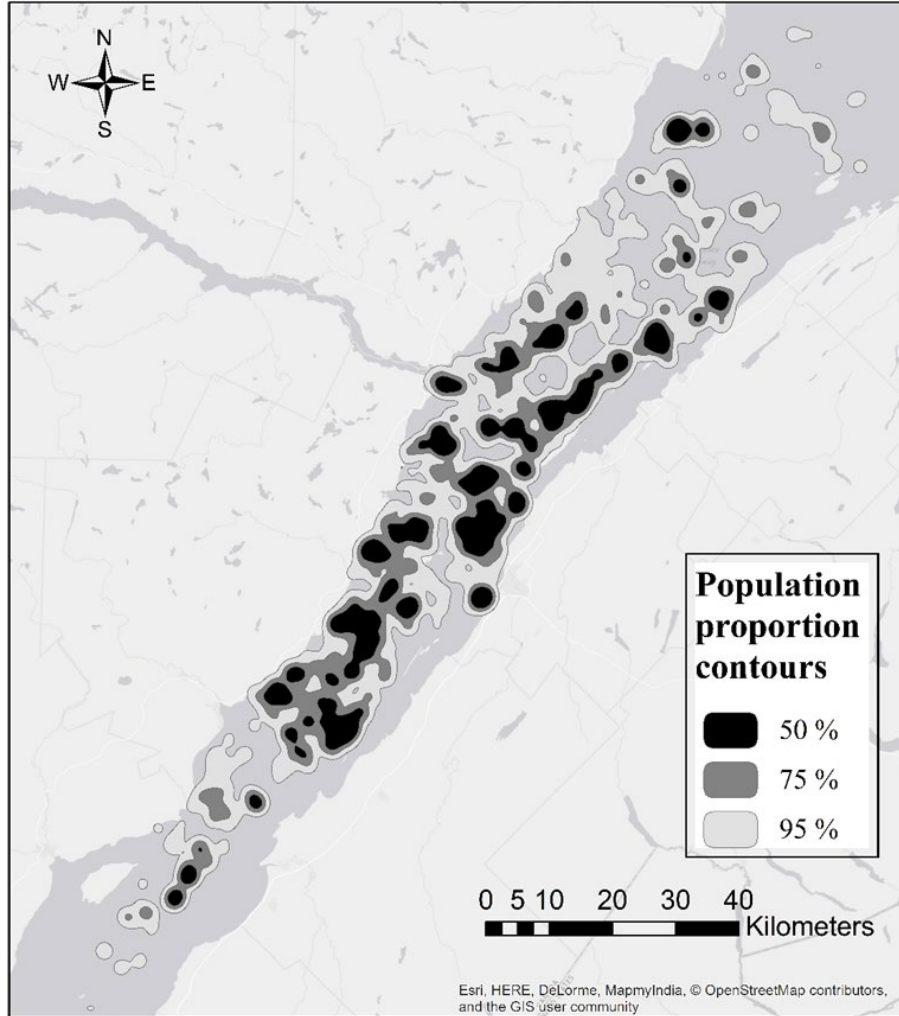


Figure 4. Areas of high density (AHD) cumulating 50, 75 and 95% of the beluga population, as defined by the kernel method, applied to data from 35 systematic aerial surveys conducted from 1990 to 2009 (modified from Mosnier et al. 2016). The 50% contour was used as a proxy for areas of consistent aggregations.

CORRECTING FOR AVAILABILITY BIAS

Event S represents the occurrence of a group of one or more beluga at or near the surface, and within field of view (McLaren 1961). Availability a is represented as (S, x) , the probability of such an occurrence at perpendicular distance x from the track-line. Availability depends on beluga surface interval and dive durations, and the amount of time a point at the water surface at distance x remains within observer view. Surface interval s and dive duration d are treated as a two-state continuous-time Markov process, and are estimated from individually tracked beluga (Laake et al. 1997), such that:

$$a(S, x) = \frac{s}{s+d} + \frac{d[1-e^{-w(x)/d}]}{s+d} \quad [\text{Eq. 1}]$$

Equation 1 is the addition of two ratios or probabilities. The first ratio estimates the mean proportion of time during a dive cycle that an animal spends at the surface or probability that an animal is at the surface when an aircraft arrives overhead. The second ratio estimates the probability of this animal appearing within an observer field-of-view during the aircraft passing,

given the probability it was diving when the aircraft arrived. This second ratio is a function of $w(x)$, the time any location at the surface at distance x remains in the observer view, given the obstructed lateral view forward and backward (\emptyset_1 and \emptyset_2 , respectively), plane speed v and perpendicular distance x of the sighting (Forcada et al. 2004; Gómez de Segura et al. 2006):

$$w(x) = \frac{x}{v} [\cot(\emptyset_1) + \cot(\emptyset_2)] \quad [\text{Eq. 2}]$$

The obstructed field-of-view forward and backward varied with aircrafts and were 30° forward and 20° backward for the Partenavia and Cessna 337, and 5° each in the case of the Twin Otter.

For photographic surveys, only the probability that an animal is at the surface when an aircraft arrives overhead is considered (i.e., first term in Eq. 1), making availability necessarily lower during photographic than visual surveys. Animals considered available to a photographic survey are those located above the turbidity threshold when the photo is taken. Availability P to photographic surveys, which represents the proportion of time spent above a defined threshold, is therefore calculated as follows:

$$P = \frac{s}{s+d} \quad [\text{Eq. 3}]$$

where s represents the time spent above, and d the time spent below a defined turbidity threshold during a dive cycle.

STATISTICAL ANALYSIS

The data set consisted of multiple geolocated dives (including dive and post-dive surface interval) from focally-tracked beluga with associated date, local time and bathymetry, and location relative to turbidity zones (1, 2, or 3) and AHD zones (inside or outside). Data were explored using standard procedures (Zuur et al. 2010) to ensure the absence of outliers or heterogeneity in the data, and of collinearity, interaction or dependency among variables.

Dependency among successive dives when examining availability as a function of covariates was accounted for by including beluga focal ID as a random intercept in generalized additive mixed-effects models (GAMM). The validity of using a GAMM (and not a generalized linear mixed model) was assessed from the effective degree of freedom of the smooth term, where an $\text{edf} > 1$ indicates a non-linear relationship. A single response variable was considered for photographic surveys, i.e., the proportion of time a beluga was available during a dive cycle [i.e., P in Eq. 3], whereas two response variables were considered for visual surveys [i.e., s and d]. Resulting functions from the two response variables were incorporated into Eq. 1 to obtain sighting-specific availability during visual surveys based on its location and associated characteristics. The relationship between residuals from the models using s and d as response variables was examined using scatterplots and Pearson correlation coefficients to ensure none existed and thus, that a multivariate model was not needed, and that incorporating functions for s and d into Eq. 1 was appropriate.

Three covariates were considered in the models: zone (1, 2, and 3), seafloor depth (included as a smooth term), and location relative to AHD (inside or outside). Julian date and time-of-the-day were also considered for inclusion, but were ultimately excluded from the models; there were concerns that the uneven coverage of daytime hours due to short deployment times and span of tagging effort over several months would increase the likelihood of a few individuals biasing seasonal and diel effects. Spatially-explicit models were also considered, but not applied to the data given that models without spatial dependency did not indicate any major spatial patterns in the residuals. Exploratory analyses revealed no interactions among the three covariates. As a

result, seven models were tested, representing all potential combinations of the three covariates, with no interaction term. The highly restricted diving depth range in several of the individuals prevented testing a model with a random intercept and random slope, i.e., with an overall and an animal-specific depth smoother.

Generalized additive mixed models were used to describe effects from environmental and behavioural features on P , s , and d in a three-step process (Figure 5). First, the potential heterogeneity in beluga surface s and dive times d as a result of the defined covariates was explored without consideration for turbidity, i.e., using 0.5 m as the threshold for defining a dive. These two response variables were continuous and positive; therefore, we used a Gamma GAMM with a log-link function. Restricted maximum likelihood (REML) was used to estimate the smoothing parameters (Wood 2018). The resulting models were defined as follows:

$$\begin{aligned}
 d_{ij} \text{ or } s_{ij} &\sim \text{Gamma}(\mu_{ij}, r) \\
 E[d_{ij}] \text{ or } E[s_{ij}] &= \mu_{ij} \\
 \text{var}[d_{ij}] \text{ or } \text{var}[s_{ij}] &= \mu_{ij}^2 / r \\
 u_{ij} &= \exp(\text{Intercept} + \text{Covariates}_{ij} + a_i) \\
 a_i &\sim N(0, \sigma^2)
 \end{aligned}$$

where d_{ij} and s_{ij} are respectively, the estimated diving and surface interval durations for animal i and j^{th} dive, r is an unknown parameter controlling the variance, and a_i is a random intercept for animal i , which is assumed to be normally distributed with mean 0 and variance σ^2 . Note that this analysis was not conducted for photographic surveys given that time s , spent at the surface above 0.5 m, was generally a second or less (i.e., 0 s) for most dives, resulting in overly small P .

The added effect of turbidity on instantaneous availability P , and on s and d was then examined as a function of the same three covariates by using 4 m as a threshold to define a dive, i.e., the average turbidity for the SLE beluga summer habitat (as in Kingsley and Gauthier 2002). Given that P is a ratio ranging from 0 to 1, a beta GAMM with a logistic link function was used in this case, such that:

$$\begin{aligned}
 P_{ij} &\sim \text{beta}(\pi_{ij}, \theta) \\
 E[P_{ij}] &= \pi_{ij} \\
 \text{var}[P_{ij}] &= \pi_{ij} * (1 - \pi_{ij}) / (1 + \theta) \\
 \text{logit}(\pi_{ij}) &= \text{Intercept} + \text{Covariates} + a_i \\
 a_i &\sim N(0, \sigma^2)
 \end{aligned}$$

where P_{ij} is the proportion of time spent at the surface for animal i and j^{th} dive, θ is an unknown parameter controlling the variance, and a_i is a random intercept for animal i , which is assumed to be normally distributed with mean 0 and variance σ^2 .

In a third step, the added effect of location-specific turbidity was examined using a composite file consisting of the data reprocessed with a 2 m, 5 m and 8 m threshold to define a dive, and from which only sightings falling within the corresponding zone of turbidity (either zones 1, 2 or 3, respectively) were extracted. Again, a beta GAMM and gamma GAMMs were applied to P (photographic surveys) and s and d (visual surveys), respectively, to examine effects of the three covariates.

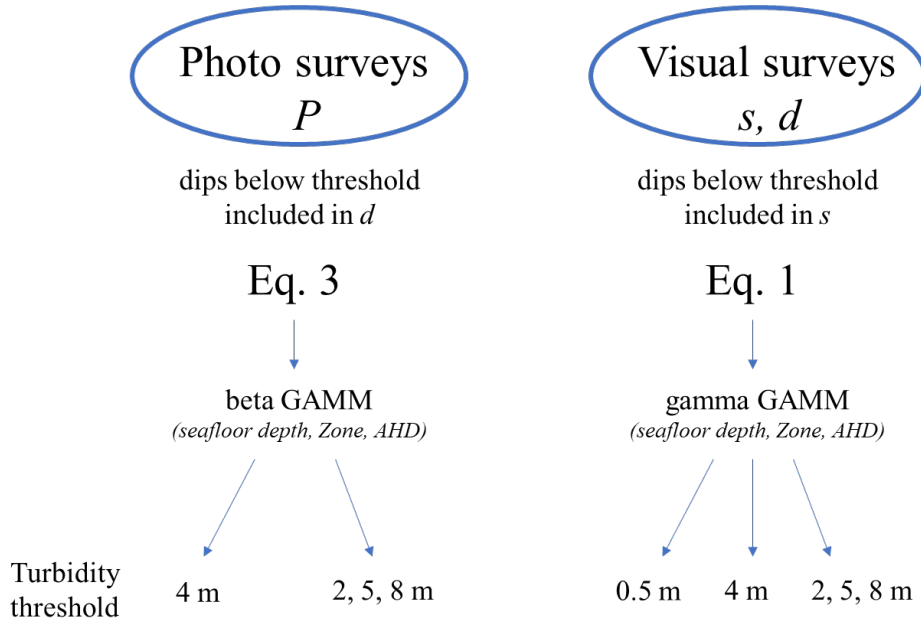


Figure 5. Analytical process for assessing effects from environmental and behavioural correlates on availability P during photographic surveys, and on surface time s and dive time d using generalized additive mixed effects models (GAMM). Zones and areas of high density (AHD; 50%) are identified in Figures 2 and 4, respectively.

Models were fitted using the *mgcv* package (v1.8-40; Wood 2011) in R software (v4.2.2, R Development Core Team 2022). The main tool to find the optimal model was the Akaike information criteria (AIC); the simpler model was selected when difference in AIC was < 2 . Model assumptions were verified by plotting Pearson residuals against fitted values, and against each covariate in the model and not in the model (Zuur et al. 2009). Spatial dependency of the residuals and the random effect was assessed using variograms (Schabenberger and Pierce 2002).

CORRECTING AVAILABILITY BIAS FOR PHOTO OVERLAP

For photographic surveys, there was a need to account for photo overlap when estimating availability. Kingsley and Gauthier (2002) developed their availability bias correction from group observations while assuming a 16 s interval and overlap of 30% between successive photos. However, interval between photos varied from 3—19 s among surveys, with an achieved photo overlap of 0 to 39% (St-Pierre et al. 2023). The probability P_D of a beluga being imaged in at least one of two photographs taken 3, 6, 16, 19, 20, and 22 s apart was therefore estimated using tag data (Supplement 3). P_D was set as the proportion of paired observations at these time intervals, where the depth reading was at or above the average turbidity threshold for the study area (i.e., 4 m) for at least one of the two observations. Availability corrected for photo overlap \bar{P} was calculated as in Kingsley and Gauthier (2002):

$$\bar{P} = \frac{(1-2V)P + VP_D}{1-V} \quad [\text{Eq. 4}]$$

where, V is the overlap, and P is the availability bias obtained from the GAMM model.

ESTIMATING GROUP SIZE AND ABUNDANCE

To estimate abundance and associated total variance, 5000 availability bias estimates were produced for each sighting according to its specific seafloor depth, Zone, AHD values using a bootstrap procedure based on posterior simulation (Wood 2018). These 5000 estimates of P or $a(S, x)$ were produced by resampling model parameters with replacement (i.e., seafloor depth, Zone, AHD and random effect). The functions relating effects from environmental variables to $a(S, x)$ via s and d in Eq. 1 required information on perpendicular distance (among other variables). The few sightings with missing perpendicular distances were allocated a geolocation using preferably double-platform observation data; if unavailable or uncertain, they were given the default value of 0 m (i.e., directly underneath the aircraft).

From the 5000 P and $a(S, x)$ per sighting were generated 5000 corrected cluster size estimates, which formed the basis for estimating 5000 abundance estimates and associated variance as per procedures described in St-Pierre et al. 2023. Corrected cluster size estimates \bar{E} were obtained from group size E as follows for photographic and visual surveys, respectively:

$$\bar{E} = E \cdot \frac{1}{\bar{P}} \text{ or } \bar{E} = E \cdot \frac{1}{a(S, x)} \quad [\text{Eq. 5}]$$

SENSITIVITY ANALYSIS

The sensitivity of availability bias to survey design, survey platform, sightings distribution, turbidity threshold and each covariate was examined using two datasets: 1) all photographic surveys conducted from 1990—2019 ($n = 11$), and 2) replicate visual surveys available from 2005 ($n = 14$). The selected values for forward and backward obstructed field-of-view (Eq. 2) for a given survey platform was examined for their influence on availability using the four replicate surveys from 2019, which is the only surveys flown with a popular platform for beluga and other cetaceans surveys in other areas, the Twin Otter.

Sensitivity analyses were conducted using the best model selected based on AIC for photographic and visual surveys (see Results).

RESULTS

Seventeen of the 44 tags deployed could not be used: one was lost, four recorded no data, three provided data solely in the Saguenay Fjord, and nine were deployed on beluga we lost sight of after tagging. Deployment duration varied among the 27 remaining tags from 0.7 to 29.8 h. Once nighttime activity and other segments of unusable data were removed, there remained an average of 4.5 h of usable data per beluga (total: 134 h), with geolocations spread among the three zones (Figure 3).

Not all individuals visited the three zones, with 9, 8, and 21 individuals visiting zones 1, 2, and 3, respectively. Seafloor depth was unevenly distributed among these zones, being deeper on average in zone 3 (Figure 3), and also deeper on average outside than inside AHD zones (95 m *versus* 37 m, respectively). Data exploration revealed no specific problems with the data, confirming its irregularly spaced nature, and an expected interindividual variability in s and d . There was no relationship between s and d , with d [but not s] increasing with seafloor depth.

Using a 0.5 m threshold to define a dive, d and s were variable among the 27 tagged individuals, averaging 176.6 s (weighted SE = 12.6 s) and 51.6 s (weighted SE = 4.5 s), respectively. Beluga dove on average for similar durations in all three zones of their summer range; however, surface times were approximately 50% longer when in the deeper zone (zone 3) than when in the other two zones (Supplement 4a).

Overall, mean availability decreased with increasing turbidity. As expected, turbidity was higher for visual than photographic surveys due to dips below the turbidity threshold being logged as part of surface time for visual surveys, although values became almost identical between photographic and visual surveys at turbidity ≥ 4 m (Supplement 4b).

DIVE TIME

Environmental correlates of beluga dive times were the same regardless of whether effects of turbidity were considered (4-m average or zone-specific) or not (0.5 m) when estimating d (Supplement 5). Specifically, variations in dive time were best explained by models including all three covariates, i.e., seafloor depth, zone, and their location relative to AHD (inside or outside). Generally, d increased with seafloor depth down to about 50 m, with mild fluctuations at deeper depths (Figure 6), and was overall longer when belugas were inside AHDs or in Zone 1 (2 m; the Upper Estuary). In all three models, a spatial dependency in Pearson residuals was noted up to approximately 400 m. The average net displacement speed for these tagged beluga (5.8 km h⁻¹; Lemieux Lefebvre et al. 2012) and mean dive durations (1.3—3.3 min depending on dive type; Lemieux Lefebvre et al. 2018) suggest that spatial dependency was greatly reduced beyond 2—3 consecutive dives or for dives performed more than 4 min apart.

SURFACE TIME

Variations observed in s were generally unrelated to covariates. Only when zone-specific turbidity was taken into account were zone or seafloor depth slightly improving the fit to the data over the intercept-only model (Supplement 6). However, the depth smoother was highly non-significant (P -value = 0.34), and the zone effect arose mainly from a difference in s between the most and least turbid zones of the study area (zones 1 and 3). Similar to d , there was a mild spatial dependency detected in Pearson residuals for s , also up to approximately 400 m, i.e., within the time frame for completing two consecutive dives.

INSTANTANEOUS AVAILABILITY (P)

When P was modulated according to local turbidity, influential covariates included seafloor depth, zone, and whether animals were inside or outside AHD. However, when using 4 m as an average threshold for visibility across the study area, the model with only seafloor depth as an influential covariate was selected as the best model (Supplement 7). Generally, instantaneous availability to a photographic survey decreased from zone 3 to 1, increased with seafloor depth, and was lower when animals were inside than outside AHDs (Figure 7).

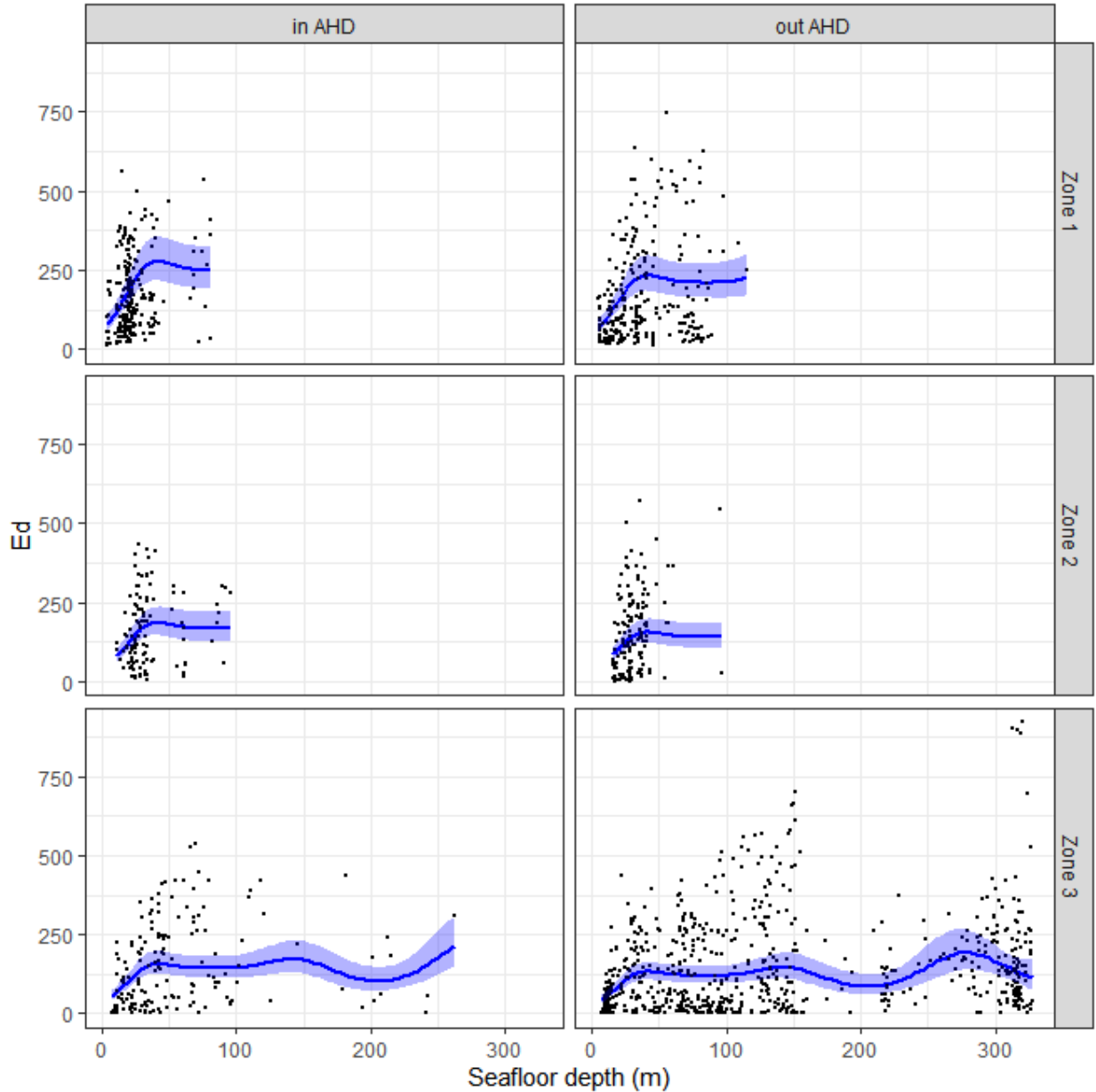


Figure 6. Dive time (E_d) with 95% confidence interval (in blue) as a function of seafloor depth (m), zone used, and whether animals were inside or outside AHD, and when considering zone-specific turbidity. Turbidity 2, 5 and 8 m correspond to Zones 1, 2 and 3, respectively.

MODEL SELECTION

The residuals from the optimal dive model d were unrelated (correlation ≤ 0.10) to the residuals of the optimal surface model s , confirming that a multivariate model for Eq. 1 was unwarranted. Given pronounced differences in turbidity across the study area, models accounting for local turbidity (2, 5 and 8 m) were deemed more appropriate for our datasets than models assuming a uniform turbidity of 4 m (Supplement 7). For photographic surveys, the selected model included seafloor depth, zone and location relative to AHDs. For visual surveys, availability was estimated using the Null model for s (Supplement 6), and a model including all three covariates for d (Supplement 5).

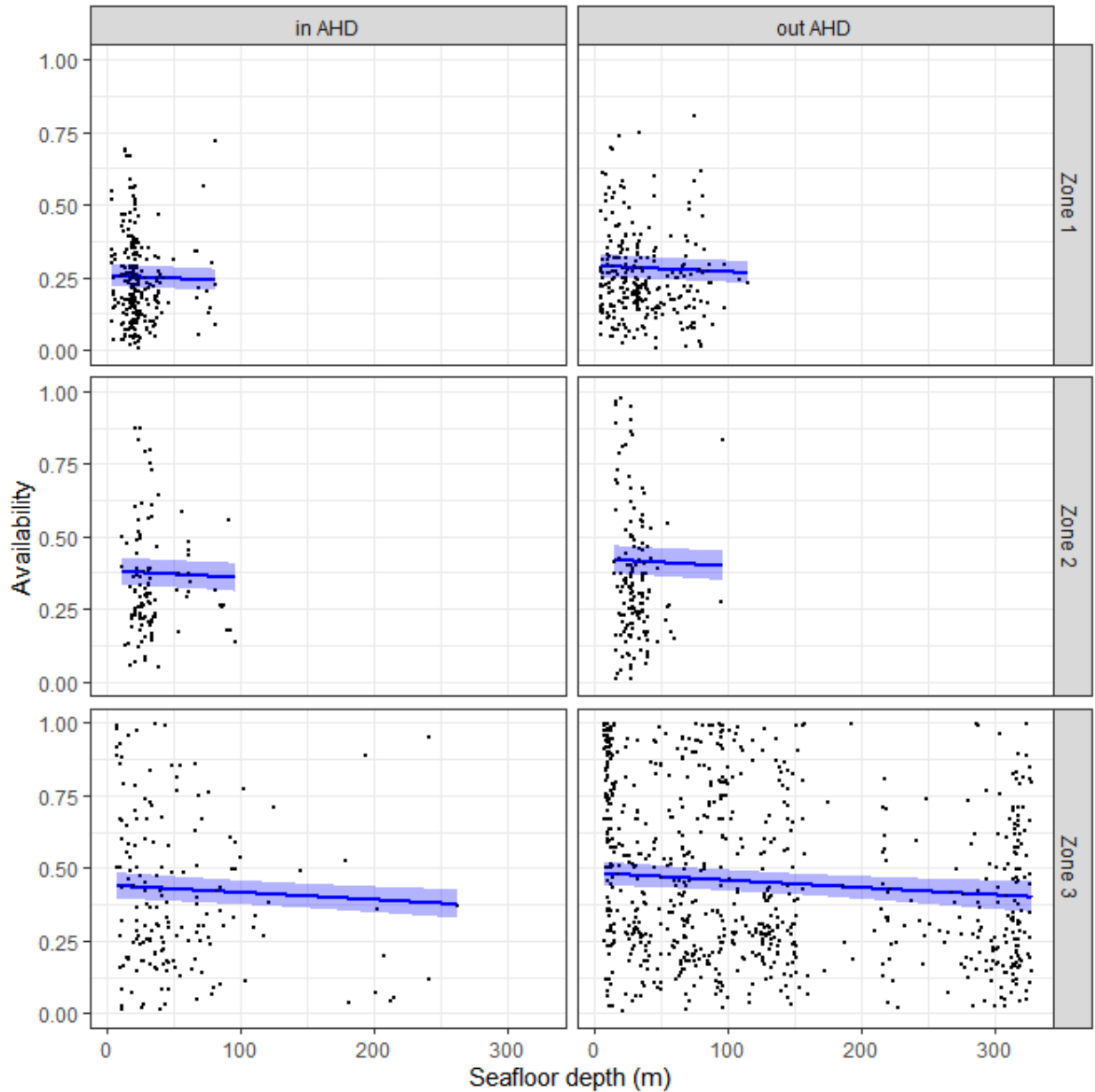


Figure 7. Instantaneous availability P with 95% confidence interval (in blue) as a function of seafloor depth (m), zone used, and whether animals were inside or outside AHD, and when considering zone-specific turbidity.

SENSITIVITY ANALYSIS

As expected from time-in-view, which is instantaneous in photographic surveys, but not visual surveys, beluga availability was on average higher during visual than photographic surveys (Figure 8). Estimates also varied more widely among observations during visual than photographic surveys (larger variance; Figure 8), likely as a result of variability in perpendicular distance and thus, time-in-view (see Eq. 1). The survey platform chosen for conducting visual surveys can strongly affect availability through their specific angles of obstructed field-of-view: the Twin Otter with a 5°-5° forward-backward obstructed view resulted in a mean availability on average 54% higher (mean of 0.763, SE = 0.10 versus 0.496, SE = 0.007) than the Partenavia

or Cessna 337 (mean 0.339, SE = 0.005), which had a 30°-20° forward-backward obstructed field-of-view (Figure 8). Using the Twin Otter and 2019 visual survey data as a test platform and dataset, with various combinations of forward-backward obstructed field-of-view further indicated that the searching pattern of observers within the available field-of-view can have a substantial impact on estimated availability: a change from a 5°-5° to a 45°-45° or 0°-90° forward-backward searching area reduced mean availability by 43—46% (Figure 9). This analysis also highlights that applying an average availability from tag data *a posteriori* to mean abundance estimates instead of including this information in Eq. 1 along with observed perpendicular distances and realistic field-of-view data, is likely to lead to an underestimation of availability and thus an overcorrection for this bias, especially for survey platforms with a wider field-of-view (Figure 9).

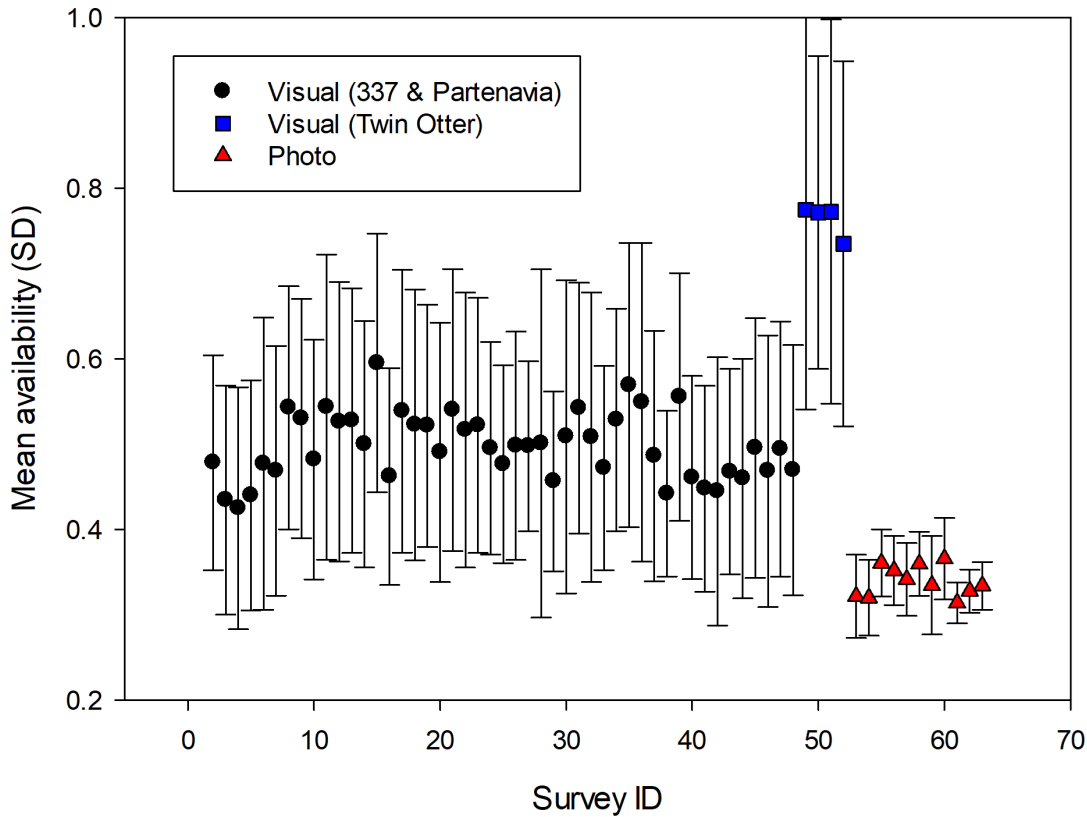


Figure 8. Mean availability (and standard deviation, SD) for all visual and photographic surveys estimated using the best identified models for estimating availability (i.e., photographic surveys: instantaneous availability is estimated while accounting for location-specific turbidity, and including as covariates the seafloor depth, zone, and location of sightings relative to areas of high densities (AHD); visual surveys: availability, which takes into account the observer's field of view, is estimated using a null model for surface time s , and one accounting for location-specific turbidity and incorporating the above three covariates for dive time d).

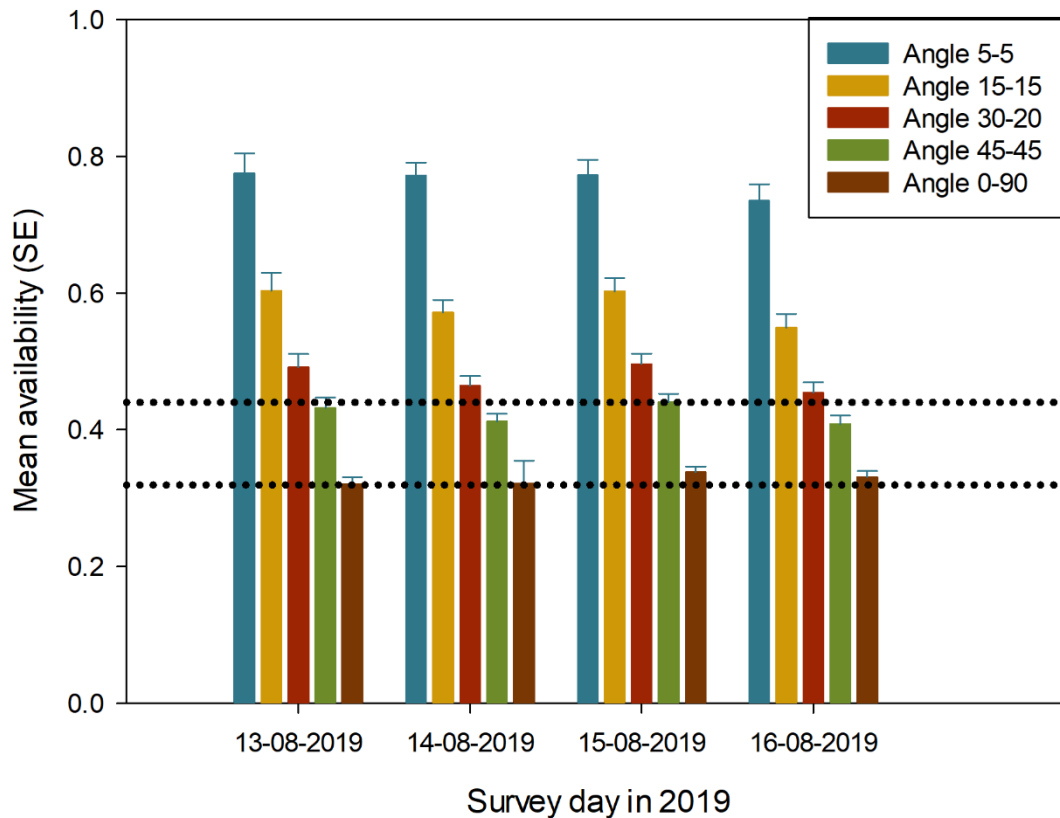


Figure 9. Effect of different combinations of forward-backward obstructed field-of-view on mean availability, illustrated using the best model for estimating availability and the four replicate visual surveys conducted using the Twin Otter in 2019. The horizontal dotted lines represents the range of mean availability to visual surveys based on the 27 tagged beluga using turbidity thresholds varying from 2 m (lower line) to 8 m (upper line) [see Supplement S4b].

Based on photographic survey data, the majority of beluga sightings are made in the zone of highest turbidity: in all but three photographic surveys (all in 2019), between 50 and 75% of the sightings were in Zone 1 (Figure 10). This zone was characterized by a lower mean availability than the other zones (0.307 versus 0.363 and 0.399 for zones 2 and 3, respectively; Figure 11). As a result, the three 2019 surveys with a higher proportion of individuals in Zones 2 and 3 showed a higher mean availability using a model accounting only for zone (258m_Zone scenario in panel (a) of Figure 12) compared to all other surveys.

Mean availability estimates varied depending on model formulation, and was generally the lowest when all three covariates were included, i.e., the best model according to AIC values. This was true for both photographic and visual surveys (Figure 12). Null models indicated that accounting for local turbidity (instead of using an average 4-m turbidity across the study area) increased availability by 2.6% and 1.6% on average for photographic and visual surveys, respectively (4m_Null versus 258m_Null scenarios in Figure 12). Model runs with location-specific turbidity (i.e., model 258m_Null) and including one covariate at a time indicated that the latent processes associated with using a specific zone had the largest effect on availability for both types of surveys (mean: -7.8% and -3.8%, respectively). While seafloor depth changed availability by less than $\pm 2\%$ in all but two [visual] surveys (mean: -0.1% and 2.0%, respectively), animals location relative to AHDs had to one exception a consistently negative effect on availability (mean: -1.7 and -2.5%, respectively).

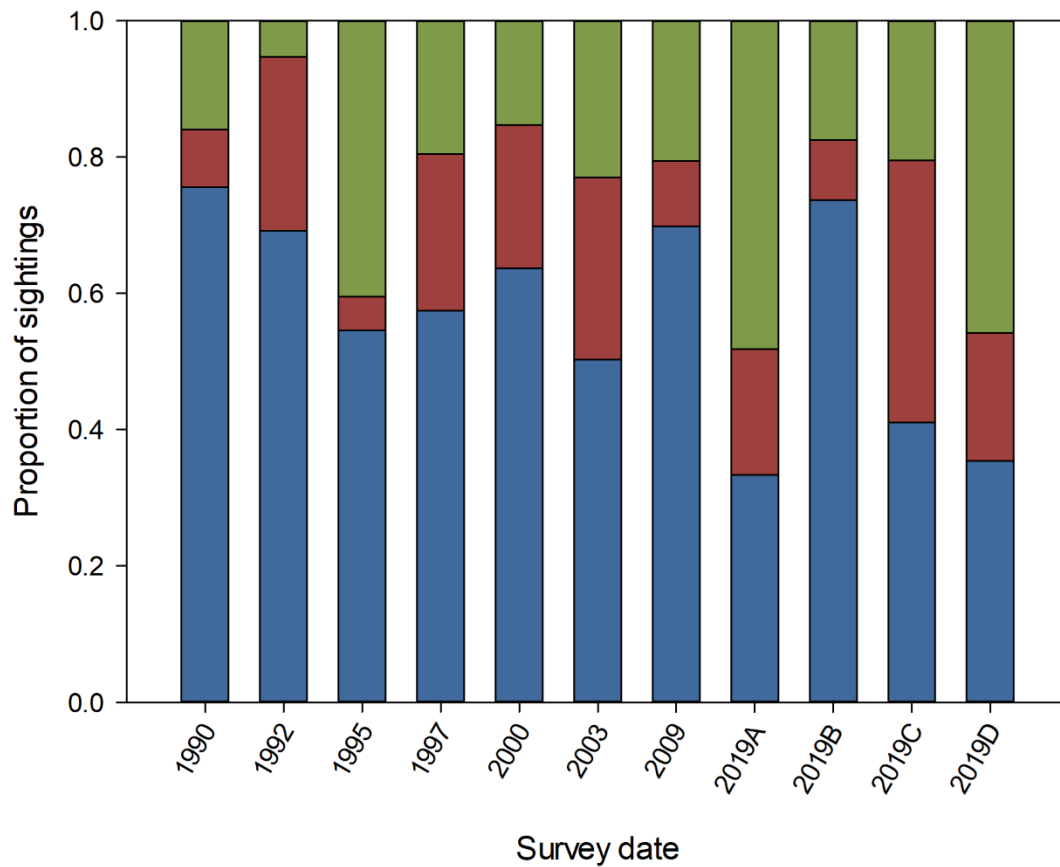


Figure 10. Distribution of beluga sightings among zones of turbidity during photographic surveys: Zone 1 (2 m; blue), Zone 2 (5 m; red) and Zone 3 (8 m; green).

Overall, accounting for all covariates and local turbidity decreased availability by an average of 6.6% for photographic surveys, i.e., from a mean of 0.363 for the Null model with a 4-m average turbidity (range 0.335—0.381), to 0.339 for the model with all three covariates and location-specific turbidity (range 0.314—0.366). Based on the 2005 sample of 14 surveys, using the full model for visual surveys decreased availability by an average of 6.0% from a mean of 0.556 for the 4-m Null model to 0.523 for the full model with location-specific turbidity (Figure 12). For a fictive population of 1000 individuals, using a 4-m Null model instead of the full model with location-specific turbidity would result on average in an under-estimation of the mean population size by approximately 190 and 115 individuals for photographic and visual surveys, i.e., roughly 20% and 10%, respectively.

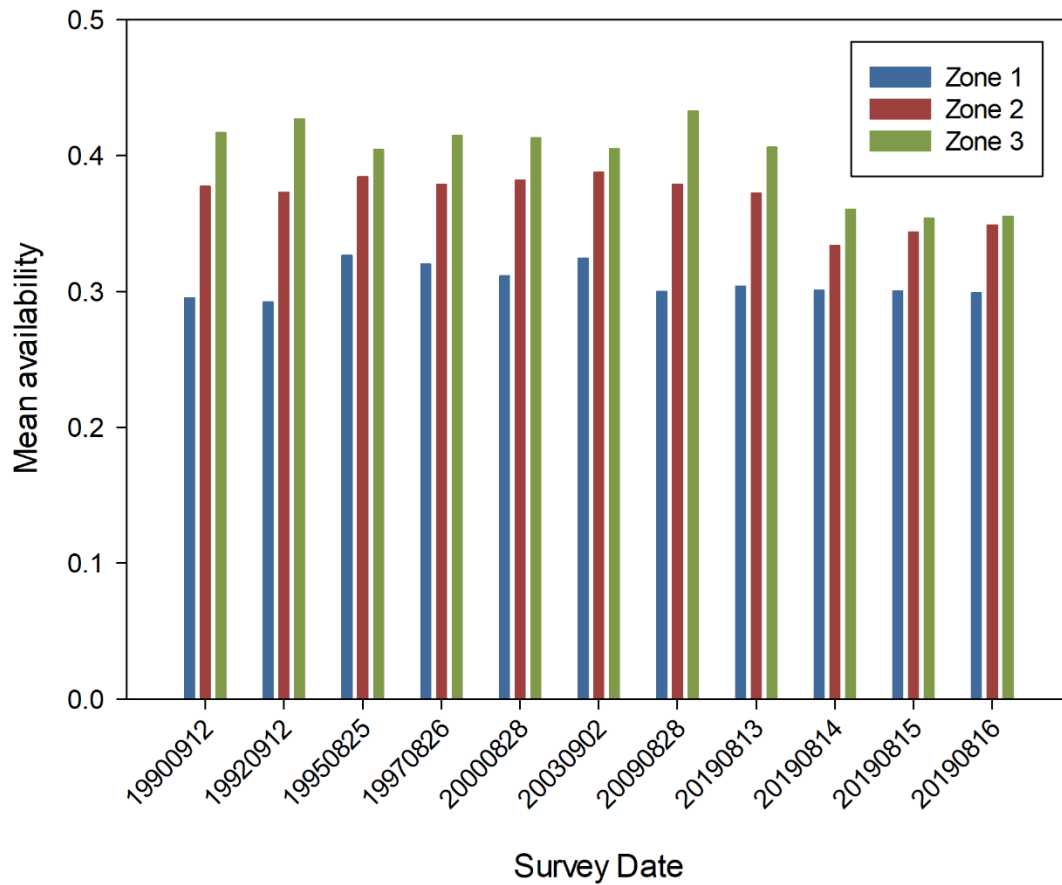


Figure 11. Mean availability per zone for the photographic surveys of St. Lawrence Estuary, as determined from the best model for availability (i.e., one that accounts for local turbidity and all three covariates).

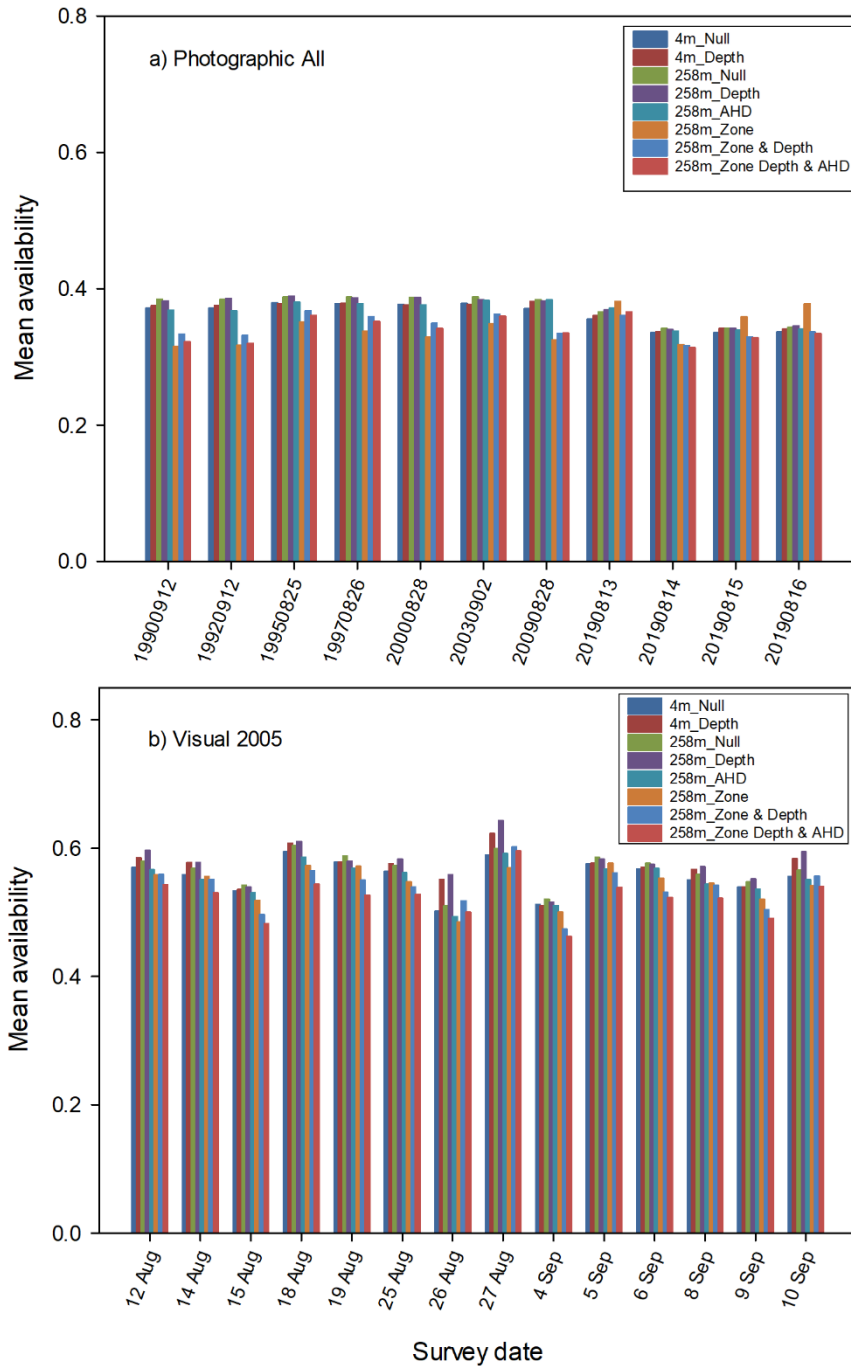


Figure 12. Mean beluga availability to a) photographic and b) visual surveys under various scenarios of local turbidity and effects of environmental or behavioural factors. Turbidity represents either the average of the study area (4 m) or is zone-specific (2, 5 or 8 m for zones 1, 2 and 3, respectively); models include either no covariates (Null), individual covariates (seafloor depth (Depth), zone (Zone) and location relative to area of high density (AHD), or their combination.

DISCUSSION

Numerous studies have estimated availability of cetaceans and other marine vertebrates to survey platforms, although few have examined the potential influence of environmental or

behavioural factors (e.g., Thomson et al. 2012; Hagihara et al. 2013; Doniol-Valcroze et al. 2015; Fuentes et al. 2015; Watt et al. 2015a; 2015b; Marcoux et al. 2016; Nykänen et al. 2018; Sucunza et al. 2018; Brown et al. 2022). This study not only provides availability estimates of SLE beluga to visual or photographic survey platforms, but also offers a comprehensive analysis of the relative influence of multiple methodological, environmental and behavioural factors on these estimates. Our results confirmed that dives are longer when animals are inside compared to outside AHDs, consistent with the prediction that these areas are used for behaviours like foraging. They also indicate that while some of the behavioural or environmental factors such as latent processes associated with the zone used may have a notable effect on availability, survey design (photographic or visual), characteristics of the survey platforms, and observer search patterns may be the most influential factors on availability bias.

As expected, availability estimates were systematically higher for visual than photographic surveys for which time-in-view is instantaneous. For visual surveys however, availability was found to be highly dependent on the defined field-of-view. Simulations for a Cessna 337 or Partenavia aircraft (see Supplement S2b) indicate that time-in-view may vary from ~ 0 s (on the trackline) to ~ 50 s within the typical observation distances for SLE beluga surveys (i.e., ~ 600 m; e.g., Gosselin et al. 2017). Time-in-view would be higher at similar distances for a Twin Otter given that the obstructed field-of-view is lower (and nearly nil) for this platform when equipped with bubble windows. This difference is confirmed by the much higher availability of beluga that we estimated for the Twin Otter. These results, and those on the sensitivity of availability estimates to the defined angles, highlight the importance of coherence between the definition of obstructed field-of-view and observer search pattern for obtaining an unbiased estimate of availability.

Availability bias corrections have been developed for different beluga populations using a variety of methods (Table 1). However, these corrections appear to have generally been applied directly to total abundance as a proportion of time available to the survey platform, without consideration for the variability of time-in-view with perpendicular distance, i.e., not using Eq. 1 (but see St-Pierre et al. 2023). Such approaches are likely to bias abundance estimates by an unknown and variable amount: a uniform but underestimated mean time-in-view would bias availability downward and abundance estimates upwards, whereas the reverse would lead to an underestimation of abundance. By not accounting for the variability in perpendicular distance when estimating availability for each observation, survey variance is also likely to be underestimated (see Figure 8).

Previous studies have highlighted the sensitivity of availability correction to turbidity for beluga surveys. In Cumberland Sound for instance, availability based on satellite telemetry data was deemed to vary from 0.224 to 0.485 for turbidity varying from 1 to 6 m, increasing abundance estimates by factors of 4.46—2.06 (e.g., Marcoux et al. 2016). Over a similar range (1.5 to 6 m), availability in the SLE changed from 0.150 to 0.343, equivalent to correction factors of 6.65—2.92 for abundance estimates. However, our modelling results indicate that correcting availability for turbidity ultimately had only a minor effect on mean availability for each survey, and that latent processes associated with each zone were instead the environmental or behavioural factor which affected availability the most. An investigation of how tides affect habitat use and diving behaviour might help further our understanding of these latent processes, including variability in foraging behaviour.

Abundance estimates for SLE beluga have been corrected previously using an availability estimate derived from observing the appearance and disappearance of groups of beluga of various size from a hovering helicopter (1—18 ind.; Kingsley and Gauthier 2002). The crude availability estimate from these experiments was 0.443 (SE = 0.038), but varied between 0.404 for areas with turbidity of 1—2 m, and 0.543 for areas with turbidity > 4 m. To account for photo

overlap (typically 30%) and the probability (P_D) of a beluga being photographed at least once on images taken 16 s apart (also typical until the 2019 survey), a corrected availability estimate (\bar{P}) of 0.478 was produced using Eq. 4 (equivalent to a correction factor of 2.09; SE = 0.16). This correction was applied previously to surface indices of both photographic and visual surveys, and assumed a uniform 4-m turbidity across the study area.

In comparison, availability bias in our study was estimated for individuals not groups. Our null model applied to photographic surveys from 1990—2019, and which considered a similar 4-m turbidity, provided an estimated availability (\bar{P}) which was consistently lower (0.336—0.379 depending on survey year; Figure 12a) than estimated by Kingsley and Gauthier (2002), even for surveys with similar overlap (30%) and intervals between frames (16 s), i.e., 1997—2003 (see St-Pierre et al. 2023). Therefore, the change in methodology for estimating availability for SLE beluga from an approach based on group visibility to one where detailed diving patterns of individuals were logged, led to a 26—42% decrease in mean availability estimates. Tagging more than one individual in a group, although challenging logistically, or examining drone videos from multiple groups could have been instructive for understanding the synchrony of surface intervals within groups and the link between the probability of detecting a group during visual surveys versus individual behaviour. It would also help comparing our results with those from Kingsley and Gauthier (2002) which focused specifically on group- and not on individual behaviour.

Whether the former study or the current one is best for estimating availability can be debated. In both studies, data collection required an aircraft or vessel to be used. While the helicopter altitude and vessel tracking distance were set to avoid behavioural reactions, a possible effect on beluga of an unknown size and direction (Senigaglia et al. 2016) cannot be ruled out. In the Kingsley and Gauthier (2002) study, a number of factors could have led to an overestimation of availability, including some identified by the authors. An overestimation of availability could arise from selecting the first sighted beluga group if these individuals were engaged in more visible behaviours. Maximum group size was defined as the maximum simultaneously seen; if not all beluga surfaced synchronously during surface intervals, then true group size was underestimated and visibility overestimated. Kingsley and Gauthier (2002) indicate that a recording session was initiated at the sight of a randomly chosen group, but provided no information as to when a session was terminated. If a session ended with the disappearance of a group and not with the initiation of a new post-dive surface interval, then surface time would be overrepresented relative to total observation time in each session, again biasing availability upwards. Finally, we noted that in Kingsley and Gauthier (2002), 75% of the observations were made in zone 1 where we found availability to be lower, but where adult males are only rarely seen during summer (Ouellet et al. 2021), suggesting a bias of the sample against a segment of the population. This potential bias is likely partly captured in the observed difference Kingsley and Gauthier noted in availability between the most turbid (likely zone 1) and least turbid areas (likely zone 3 where males are most often encountered; Ouellet et al. 2021), and where their estimated availability was 0.404 and 0.543, respectively. However, the turbidity effect itself should be relatively minor based on our results compared to the zone effect *per se*.

In our study, a larger and more evenly distributed sample among zones (sample size for zones 1 and 2 was < 0.5 that of zone 3), ideally included in a spatial model, would have been desirable. A sensitivity analysis using coastal dolphins indicated that availability was unlikely to have been biased by our sample size (27 beluga), but that an increase in sample size would have reduced variance further (Brown et al. 2022). While beluga tagging effort covered a large portion of the summer distribution of SLE beluga, it did not reach the two extremities of the SLE (Figure 3). There were also few individuals using zone 3 that were sampled while over the Laurentian Channel where bottom depth can reach more than 300 m (many were in the

shallower waters at the head of the channel). Beluga can reach depths of up to 1 000 m in other areas (Citta et al. 2013) and thus, are not limited by bottom depth in the SLE. Beluga include benthic prey in their diet in the SLE (Vladykov 1946; Lesage 2021), and are expected to feed on the bottom at least in some of the AHD identified (Mosnier et al. 2016). In our study, dive duration increased with bottom depth, although the effect of bottom depth and of being in an AHD on availability appeared relatively weak in our analysis. Given that 13—35% of the beluga may use the deep and clear waters of the Laurentian Channel at any one time (Michaud 1993), increasing sample size for this region within zone 3 might enhance the relationship between availability and bottom depth and alter modelled estimates of availability. There is currently no information leading us to believe that beluga distribution or habitat use has changed since the tagging study in the early 2000s. However, the extension of the tagging study to more recent years would confirm dive patterns and habitat use have remained consistent over time.

Another caveat of our study is related to not having sampled all age- and sex classes: females with newborn calves were required by research permit to be avoided. In other species such as coastal dolphin, this segment of the population is more available than others to survey platforms (by diving less often or to shallower depths; Brown et al. 2022); not including it may bias availability downward.

For both photographic and visual surveys, a model that accounted for all three covariates best fitted the data. The latent processes associated with using a specific zone was the covariate influencing the most availability, mainly due to the majority of sightings being made in zone 1 where availability was the lowest. Zone 1 is used almost exclusively by females with calves and juveniles during summer (Michaud 1993; Ouellet et al. 2021) for a variety of behaviours. Reasons for their lesser availability while in this zone compared to others ones -- once turbidity was accounted for -- remain unclear given the lack of understanding of the occurrence and characteristics of beluga behavioural patterns in the various zones.

An experiment in the SLE using grey and white beluga models has determined that white adults can be seen at Secchi-disk depth while grey juveniles can be seen on the film only at 50% or less of Secchi-disk depth (Kingsley and Gauthier 2002). Similar results were obtained in the Arctic, where grey juveniles could only be seen at depths half that of adults, and dark-grey neonate models, not even at 20% of an adult depth (Richard et al. 1994). This means that grey juveniles might be under-represented on photographs by an unknown amount, leading to an underestimation of abundance. This bias might be less in zone 3 where young and darker juveniles are less likely to be seen than in zone 1 and 2 (Michaud 1993; Ouellet et al. 2021). This aspect could be examined further by looking at differences in diving behaviour of grey versus white individuals in the different zones, and by estimating the proportion of these classes in the population at the time surveys are conducted. High contrast imagery is often used during photographic surveys to increase the chance of detecting animals just below the water surface. For SLE beluga surveys, most animals appear white on this high contrast imagery, limiting its use to estimate the proportion of grey versus white animals in the population.

Light reflectance at the water surface may also affect the capacity of observers to detect beluga underwater. This effect is likely to increase with distance of sightings from the aircraft, and may be more important early and late in the day when the sun is lower, or in higher Beaufort conditions. The short duration of inter-breath intervals observed in SLE beluga is, however, likely to limit this effect, especially at these longer distances from the aircraft where time-in-view is also longer (Appendix 2).

We conclude that previous estimates of SLE beluga abundance were likely biased downward by an overestimation of beluga availability and oversight of the uneven distribution of beluga among different zones with specific but undefined underlying processes. While the mean

correction factor used in the past for visual surveys was generally similar to the mean estimates obtained from the current study except when, for 2019 surveys using the Twin Otter, they were likely biased by various amounts as a result of not accounting for specific characteristics of the survey platform and the sighting's perpendicular distance from the trackline. Overall, the availability estimates obtained through the current study are likely to improve the accuracy of abundance estimates for the SLE beluga population, and to reduce differences between photographic and visual survey estimates over the time series (St-Pierre et al. 2023). For photographic and visual surveys to be fully comparable, visual surveys will also need to be corrected for perception bias.

Table 1. Correction factors for availability bias that were developed in previous studies. None of these were applied using Eq. 1.

Method	Data acquired	Study location	Availability	Reference	Comments
Visual observations (fixed-wing aircraft)	% time visible at surface	Mouth of Churchill River	≈ 0.330	Sergeant 1973	In fairly turbid waters
Archival tag	Surface and dive data	Devon Is.	0.390	Heide-Jørgensen et al. 1998	-
Archival tag	Surface and dive data	Devon Is. Cumberland Sd Sommerset Is.	0.449 0.516 0.538	Heide-Jørgensen et al. 2001	-
Archival tag	% time visible at surface	Cunningham Inlet	0.400-0.555	Martin and Smith 1992	-
Archival tag	% time visible at surface	Cumberland Sound	0.423-0.424	Richard 2013	-
Visual observations (helicopter)	% time visible at surface	St. Lawrence Estuary	0.443	Kingsley and Gauthier 2002	Observation of appearance and disappearance of individuals within groups (n = 72 groups)
Archival tag	% time visible at surface	Clearwater fjord North and West Strata (Cumberland Sound)	0.224-0.725* 0.148-0.413*	Marcoux et al. 2016	Areas contrasting by bathymetry
Radio-telemetry	Surface and dive data	Kvichak Bay	0.364**	Frost et al. 1985	
Video recording	Surface and dive data	Cook Inlet	0.493	Hobbs et al. 2000	
Satellite telemetry	Surface and dive data	Eastern Beaufort Sea	0.397-0.471***	Marcoux et al., DFO unpubl. data prep.	

Method	Data acquired	Study location	Availability	Reference	Comments
Archival tag	Surface and dive data	St. Lawrence Estuary	0.425-0.595 [†] 0.734-0.775 [§]	This study	
Archival tag	Surface and dive data	St. Lawrence Estuary	0.314-0.366	This study	

* For turbidity thresholds of 1 to 6 m

** Based on 2 beluga with very different surface times; assumed 10 s viewing time at altitude of 300 m

*** For turbidity thresholds of 1 to 5 m

[†] Assuming a 30°-20° forward-backward obstructed field of view (Cessna 337 and Partenavia P68C with bubble windows)

[§] Assuming a 5°-5° forward-backward obstructed field of view (de Havilland Twin Otter 300 with bubble windows)

ACKNOWLEDGEMENTS

We would like to thank Thomas Doniol-Valcroze, Garry Stenson and Cortney Watt for their inputs on earlier data analysis. We thank Michel Moisan and other members of the Group of Research and Education on Marine Mammals for their help with tag deployment. This project was made possible via the Species at Risk and Whale Initiative programs of Fisheries and Oceans Canada.

REFERENCES CITED

- Blane, J. M. and Jaakson, R. 1994. The impact of ecotourism boats on the St Lawrence beluga whales. *Env. Conserv.*, 21: 267-269.
- Brown, A.M., Allen, S.J., Kelly, N., and Hodgson, A.J. 2022. [Using Unoccupied Aerial Vehicles to estimate availability and group size error for aerial surveys of coastal dolphins](#). *Remote Sens. Ecol. Conserv.*
- Buckland, S. T., Anderson, D. R., Burnham, K. P., Laake, J. L., Borchers, D. L., and Thomas, L. 2004. *Advanced distance sampling: Estimating abundance of biological populations*, Oxford University Press, Oxford, UK.
- Citta, J. J., Suydam, R. S., Quakenbush, L. T., Frost, K. J., and O’Corry-Crowe, G. M., 2013. Dive behaviour of Eastern Chukchi beluga whales (*Delphinapterus leucas*), 1998-2008. *Arctic*, 66: 389-406.
- Costa, D.P., and Gales, N.J. 2003. Energetics of a benthic diver: seasonal foraging ecology of the Australian sea lion, *Neophoca cinerea*. *Ecol. Monogr.* 73: 27-43.
- Dombroski, J.R.G., Parks S.E, and Nowacek, D.P. 2021. Dive behavior of North Atlantic right whales on the calving ground in the Southeast USA: implications for conservation. *Endang. Sp. Res.* 46: 35-48.
- Doniol-Valcroze, T., Lesage, V., Giard, J., and Michaud, R. 2011. Optimal foraging theory predicts diving and feeding strategies of the largest marine predator. *Behav. Ecol.*, 22: 880-888.
- Doniol-Valcroze, T., Gosselin, J.-F., Pike, D., Lawson, J., Asselin, N., Hedges, K., and Ferguson, S. H 2015. [Abundance estimates of narwhal stocks in the Canadian high-Arctic in 2013](#). DFO Can. Sci. Advis. Sec. Res. Doc. 2015/060. v + 36 p.

-
- Forcada, J., Gazo, M., Aguilar, A., Gonzalvo, J., and Fernández-Contreras, M. 2004. Bottlenose dolphin abundance in the NW Mediterranean: Addressing heterogeneity in distribution. *Mar. Ecol. Prog. Ser.*, 275: 275-287.
- Frost, K. J., Lowry, L. F., and Nelson, R. R. 1985. Radio-tagging studies of Belukha whales (*Delphinapterus leucas*) in Bristol Bay, Alaska. *Mar. Mammal. Sci.*, 1: 191-202.
- Fuentes, M. M. P. B., Bell, I., Hagihara, R., Hamann, M., Hazel, J., Huth, A., Seminoff, J. A., Soltzick, S., and Marsh, H. 2015. Improving in-water estimates of marine turtle abundance by adjusting aerial survey counts for perception and availability biases. *J. Exp. Mar. Biol. Ecol.*, 471: 77-83.
- Gauthier, I., 1999. Estimation de la visibilité aérienne des bélugas du Saint-Laurent et les conséquences pour l'évaluation des effectifs (Master's thesis). Université du Québec à Rimouski, 104 p.
- Gómez de Segura, A., Tomás, J., Pedraza, S. N., Crespo, E. A., and Raga, J. A. 2006. Abundance and distribution of the endangered loggerhead turtle in Spanish Mediterranean waters and the conservation implications. *Anim. Conserv.*, 9: 199-206.
- Gosselin, J.-F., Hammill, M. O., and Lesage, V. 2007. [Comparison of photographic and visual abundance indices of belugas in the St. Lawrence Estuary in 2003 and 2005](#). DFO Can. Sci. Advis. Sec. Res. Doc. 2007/025. ii + 27 p.
- Gosselin, J.-F., Hammill, M. O., and Mosnier, A. 2014. [Summer abundance indices of St. Lawrence Estuary beluga \(*Delphinapterus leucas*\) from a photographic survey in 2009 and 28 line transect surveys from 2001 to 2009](#). DFO Can. Sci. Advis. Sec. Res. Doc. 2014/021. iv + 51 p.
- Gosselin, J.-F., Hammill, M. O., Mosnier, A., and Lesage, V. 2017. [Abundance index of St. Lawrence Estuary beluga, *Delphinapterus leucas*, from aerial visual surveys flown in August 2014 and an update on reported deaths](#). DFO Can. Sci. Advis. Sec. Res. Doc. 2017/019. v + 28 p.
- Hagihara, R., Jones, R. E., Grech, A., Lanyon, J. M., Sheppard, J. K., and Marsh, H. 2013. Improving population estimates by quantifying diving and surfacing patterns: A dugong example. *Mar. Mamm. Sci.*, 30: 348-366.
- Heide-Jørgensen, M. P., Richard P. R. and Rosing-Asvid, A. 1998. Dive patterns of belugas (*Delphinapterus leucas*) in waters near Eastern Devon Island. *Arctic*, 51: 17-26.
- Heide-Jørgensen, M. P., Hammeken, N., Dietz, R., Orr, J., and Richard, P. R. 2001. Surfacing times and dive rates for narwhals (*Monodon monoceros*) and belugas (*Delphinapterus leucas*). *Arctic*, 54: 284-298.
- Higdon, J.W., and Ferguson, S.H. 2017. Database of aerial surveys and abundance estimates for beluga whales (*Delphinapterus leucas*) and narwhals (*Monodon monoceros*) in the Canadian Arctic. *Can. Tech. Rep. Fish. Aquat. Sci.* 3211: v + 48 p.
- Hobbs, R. C., Waite, J. M., and Rugh, D. J. 2000. Beluga, *Delphinapterus leucas*, group sizes in Cook Inlet, Alaska, based on observer counts and aerial video. *Mar. Fish. Rev.*, 62: 46-59.
- Kingsley, M. C. S., 1998. Population index estimates for the St. Lawrence belugas, 1973-1995. *Mar. Mammal Sci.*, 14: 508-530.
- Kingsley, M. C. S., 2002. Status of the belugas of the St. Lawrence Estuary, Canada. *NAMMCO Sci. Publ.*, 4: 239-257.
-

-
- Kingsley, M. C. S. and Gauthier, I. 2002. Visibility of St. Lawrence belugas to aerial photography, estimated by direct observation. *NAMMCO Sci. Publ.*, 4: 259-270.
- Kingsley, M. C. S. and Hammill, M. O. 1991. Photographic census surveys of the St. Lawrence beluga population, 1988 and 1990. *Can. Tech. Rep. Fish. Aquat. Sci.*, 1776: 19 p.
- Laake, J. L., and Borchers, D. L. 2004. Methods for incomplete detection at distance zero. pp. 108-189, *In* *Advanced Distance Sampling* (S. T. Buckland, D. R. Anderson, K. P. Burnham, J. L. Laake, D. L. Borchers and L. Thomas, eds. Oxford University Press, Oxford, U.K.
- Laake, J. L., Calambokidis, J., Osmek, S. D., and Rugh, D. J. 1997. Probability of detecting harbor porpoise from aerial surveys: Estimating $g(0)$. *J. Wildl. Manag.*, 61: 63-75.
- Langton, S. D., Collett, D., and R. Sibly, M. 1995. Splitting behaviour into bouts: A maximum likelihood approach. *Behaviour*, 132: 781-799.
- Lemieux Lefebvre, S., Michaud, R., Lesage, V., and Berteaux, D. 2012. Identifying high residency areas of the threatened St. Lawrence beluga whale from fine-scale movements of individuals and coarse-scale movements of herds. *Mar. Ecol. Prog. Ser.*, 450: 243-257.
- Lemieux Lefebvre, S., Lesage, V., Michaud, R., and Humpfries, M. 2018. Combining herd surface activities with individual dive profiles to classify behaviours in beluga from the St. Lawrence Estuary, Canada. *Can. J. Zool.* 96: 393-410.
- Lesage, V. 2021. The challenges of a small population exposed to multiple anthropogenic stressors and a changing climate: the St. Lawrence Estuary beluga. *Polar Res.* 2021, 40: 5523.
- Lowry, L.F., Citta, J., O'corry-Crowe, G., Quakenbush, L.T., Frost, K.J., Suydam, R., Hobbs, R.C., and Gray, T. 2019. Distribution Abundance Harvest and Status of Western Alaska Beluga. *Mar. Fish. Rev.* 81: 54-71.
- Luque, S. P., 2007. Diving behaviour analysis in R. *R News*, 7: 8-14.
- Luque, S. P. and Guinet, C. 2007. A maximum likelihood approach for identifying dive bouts improves accuracy, precision, and objectivity. *Behaviour*, 144: 1315-1332.
- Marcoux, M., Young, B. G., Asselin, N. C., Watt, C. A., Dunn, J. B., and Ferguson, S. H. 2016. [Estimate of Cumberland Sound beluga \(*Delphinapterus leucas*\) population size from the 2014 visual and photographic aerial survey](#). DFO Can. Sci. Advis. Sec. Res. Doc. 2016/037. iv + 19 p.
- Marsh, H. and Sinclair, D. F. 1989. Correcting for visibility bias in strip transect aerial surveys of aquatic fauna. *J. Wildl. Manag.*, 53: 1017-1024.
- Martin, A. R. and Smith, T. G. 1992. Deep diving in wild, free-ranging beluga whales, *Delphinapterus leucas*. *Can. J. Fish. Aquat. Sci.*, 49: 462-466.
- Martin, A. R. and Smith, T. G. 1999. Strategy and capability of wild belugas, *Delphinapterus leucas*, during deep, benthic diving. *Can. J. Zool.*, 77: 350-360.
- McLaren, I. A., 1961. Methods of determining the numbers and availability of ringed seals in the eastern Canadian Arctic. *Arctic*, 14: 162-175.
- Michaud, R. 1993. Distribution estivale du béluga du Saint-Laurent; synthèse 1986 à 1992. *Rapp. Tech. Can. Sci. Halieut. Aquat.*, 1906: vi + 28 p.
- Michaud, R. 2005. Sociality and ecology of the odontocetes. In Ruckstuhl, K. E. and P. Neuhaus (eds) *Sexual segregation in vertebrates: Ecology of the two sexes*, Cambridge University Press, Cambridge, UK, p. 303-326.
-

-
- Mosnier, A., Lesage, V., Gosselin, J.-F., Lemieux Lefebvre, S., Hammill, M. O., and Doniol-Valcroze, T. 2010. [Information relevant to the documentation of habitat use by St. Lawrence beluga \(*Delphinapterus leucas*\), and quantification of habitat quality](#). DFO Can. Sci. Advis. Sec. Res. Doc. 2009/098. iv + 35 p.
- Mosnier, A., Doniol-Valcroze, T., Gosselin, J.-F., Lesage, V., Measures, L. N., and Hammill, M. O. 2015. Insights into processes of population decline using an integrated population model: The case of the St. Lawrence Estuary beluga (*Delphinapterus leucas*). *Ecol. Model.*, 314: 15-31.
- Mosnier, A., Larocque, R., Lebeuf, M., Gosselin, J.-F., Dubé, S., Lapointe, V., Lesage, V., Lefavre, D., Senneville, S., and Chion, C. 2016. [Définition et caractérisation de l'habitat du béluga \(*Delphinapterus leucas*\) de l'estuaire du Saint-Laurent selon une approche écosystémique](#). Secr. Can. de consult. sci. du MPO. Doc. de rech. 2016/052. vi + 93 p.
- Nykanen, M., Jessopp, M., Doyle, T. K., Harman, L. A., Cañadas, A., Breen, P., Hunt, W., Mackey, M., Cadhla, O. Ó., Reid D., and Rogan, E. 2018. Using tagging data and aerial surveys to incorporate availability bias in the abundance estimation of blue sharks (*Prionace glauca*). *PLoS One*, 13(9): e0203122.
- Ogeret, F., Cox, S.L., Weimerskirch, J., and Guinet, C. 2019. Body condition influences ontogeny of foraging behavior in juvenile southern elephant seals. *Ecol. Evol.* 9: 223–236.
- Ouellet, J.-F., Michaud, R., Moisan, M., and Lesage, V. 2021. Estimating the proportion of a beluga population using specific areas from connectivity patterns and abundance indices. *Ecosphere* 12:e03560
- Pollock, K., Marsh, H., Lawler, I. R., and Aldredge, M. W. 2006. Estimating animal abundance in heterogeneous environments: An application to aerial surveys for dugongs. *J. Wildl. Manag.*, 70: 255-262.
- R Development Core Team. 2022. [R: A language and environment for statistical computing](#). R Foundation for Statistical Computing, Vienna, Austria.
- Richard, P.R., Weaver, P.A., Dueck, L. and Barber, D.A. 1994. Distribution and relative abundance of Canadian high Arctic narwhals (*Monodon monoceros*) in August 1984. *Meddr Grønland, Biosci.* 39:41-50.
- Richard, P. R. 2013. [Size and trend of the Cumberland Sound beluga whale population, 1990 to 2009](#). DFO Can. Sci. Advis. Sec. Res. Doc. 2012/159. iii + 28 p.
- Schabenberger, O., and Pierce, F. 2002. Contemporary statistical models for the plant and soil sciences. CRC Press, Boca Raton, 760 p.
- Schreer, J.F., and Kovacs, K.M. 1997. Allometry of diving capacity in air-breathing vertebrates. *Can. J. Zool.* 75: 339-358.
- Senigaglia, V., Christiansen, F., Bejder, L., Gendron, D., Lundquist, D., Noren, D.P., Schaffar, A., Smith, J.C., Williams, R., Martinez, E., Stockin, K., and Lusseau, D. 2016. Meta-analyses of whale-watching impact studies: comparisons of cetacean responses to disturbance. *Mar. Ecol. Prog. Ser.* 542: 251-263.
- Sergeant, D. E., 1973. Biology of white whales (*Delphinapterus leucas*) in Western Hudson Bay. *J. Fish. Res. Board Can.*, 30: 1065-1090.
- Stenson, G.B., Hammill, M.O., Lawson, J.W., and Gosselin, J.-F. 2014. [Estimating pup production of Northwest Atlantic Harp Seals, *Pagophilus groenlandicus*, in 2012](#). DFO Can. Sci. Advis. Sec. Res. Doc. 2014/057.
-

-
- St-Pierre, A.P., Lesage, V., Mosnier, A., Tinker, M.T., Gosselin, J.-F. 2024. [Summer Abundance Estimates for St. Lawrence Estuary Beluga \(*Delphinapterus leucas*\) from 52 Visual Line Transect Surveys and 11 Photographic Surveys Conducted from 1990 to 2022](#). DFO Can. Sci. Advis. Sec. Res. Doc. 2023/048. v + 82 p.
- Sucunza, F., Danilewicz, D., Cremer, M., Andriolo, A., and Zerbini, A. N. 2018. Refining estimates of availability bias to improve assessments of the conservation status of an endangered dolphin. PLoS one, 13: e0194213.
- Taylor, B. L., Martinez, M., Gerrodette, T., and Barlow, J. 2007. Lessons from monitoring trends in abundance of marine mammals. Mar. Mammal Sci., 23: 157-175.
- Thomas, L., Buckland, S. T., Rexstad, E. A., Laake, J. L., Strindberg, S., Hedley, S. L., Bishop, J. R. B., Marques, T. A., and Burnham, K. P. 2010. Distance software: Design and analysis of distance sampling surveys for estimating population size. J. Appl. Ecol., 47: 5-14.
- Thomson, J. A., Cooper, A. B., Burkholder, D. A., Heithaus, M. R., and Dill, L. M. 2012. Heterogeneous patterns of availability for detection during visual surveys: Spatiotemporal variation in sea turtle dive-surfacing behaviour on a feeding ground. Methods Ecol. Evol., 3: 378-387.
- Vladykov, V. D., 1946. Études sur les mammifères aquatiques. IV. Nourriture du marsouin blanc (*Delphinapterus leucas*) du fleuve et du golfe Saint-Laurent. Department of Fisheries, Province of Quebec, 129 p.
- Watt, C.A., Marcoux, M., Asselin, N. C., Orr, J. R., and Ferguson, S. H. 2015a. [Instantaneous availability bias correction for calculating aerial survey abundance estimates for narwhal \(*Monodon monoceros*\) in the Canadian High Arctic](#). DFO Can. Sci. Advis. Sec. Res. Doc. 2015/044. v + 13 p.
- Watt, C. A., Marcoux, M., Leblanc, B., and Ferguson, S. H. 2015b. [Instantaneous availability bias correction for calculating aerial survey abundance estimates for bowhead whales \(*Balaena mysticetus*\) in the Canadian High Arctic](#). DFO Can. Sci. Advis. Sec. Res. Doc. 2015/046. vi + 21 p.
- Whitehead, H. and Weilgart, L. 1991. Patterns of visually observable behaviour and vocalizations in groups of female sperm whales. Behaviour, 118: 275-296.
- Wood, S. N. 2011. Fast stable restricted maximum likelihood and marginal likelihood estimation of semiparametric generalized linear models. J. Royal Statist. Soc. Ser. B Statist. Methodol., 73: 3–36.
- Wood, S.N. 2018. Generalized Additive Models: An Introduction with R (2nd Edition). Chapman & Hall/CRC, Boca Raton.
- Zuur, A.F., Ieno, E.N., Walker, N., Saveliev, A.A., and Smith, G.M. 2009. Mixed effects models and extensions in ecology. Springer, New York.
- Zuur, A.F., Ieno, E.N., and Elphick, C.S. 2010. A protocol for data exploration to avoid common statistical problems. Methods Ecol. Evol. 1: 3–14.

APPENDIX 1. TURBIDITY GRADIENT IN THE ST. LAWRENCE ESTUARY.



Figure A1. Satellite image of the St. Lawrence Estuary (29 August 2014) showing the water turbidity gradient from high turbidity in the Upper Estuary (west of the Saguenay River) to clear water in the Lower Estuary and the Laurentian Channel (east of the Saguenay River). Source: Rapid Response imagery, LANCE/NASA/GSFC/Earth Science Data and Information System (ESDIS).

APPENDIX 2. EFFECTS OF DIPS BELOW TURBIDITY THRESHOLD DURING SURFACE INTERVALS ON AVAILABILITY TO VISUAL SURVEYS

Dips below turbidity thresholds were observed in more than half the dives performed in Zone 1, the high turbidity zone, but nearly none of the dives from the other two zones (Table A2). Dips were also on average longer in turbid compared to clearer waters.

Simulations using plane speed (100 knots) and angle for field-of-view (30 degrees forward and 20 degrees backward) typical of SLE beluga visual survey planes (Cessna 337 and Partenavia) indicate that these dips have little effects on beluga availability to an observer, even in zones where turbidity is maximal. Dips remained overall short compared to the time available to an observer for detection. Using mean dip time per breath (3.6 s) and surface interval duration from the highest turbidity zone (67 s) as an extreme example, simulations indicate that distance-in-view (i.e., the maximum distance from the 30° deg at the front and 20° at the back, that you can see at perpendicular distance x) increases rapidly with perpendicular distance (Figure A2a), with time-in-view remaining above dip time at virtually all perpendicular distances (Figure A2b). Given the asymptotical increase in availability with time-in-view (Figure A2c), the latter would need to be less than 7 or 8 s for the correction factor to deviate from 1.00. Even if beluga were directly on the trackline where time-in-view was near zero, chances of detecting the beluga would still be 0.95 or more.

We conclude that dip time was small compared to time-in-view even in the zone of highest turbidity, with very little chance (correction factor of 0.95 to 1.00) for an animal to NOT become available to an observer during the plane overpass.

Table A2. Mean duration of dips below different turbidity thresholds presented relative to mean breath and surface interval durations.

Turbidity threshold (m)	% dives with dips below threshold	% surface interval spent below threshold	Time (in s) during a breath spent below threshold	Surface interval duration (in s) (including dips)
2	60	12	3.6	67
4	22	2	1.6	78
5	12	1	0.8	78
8	1	0	0.1	86

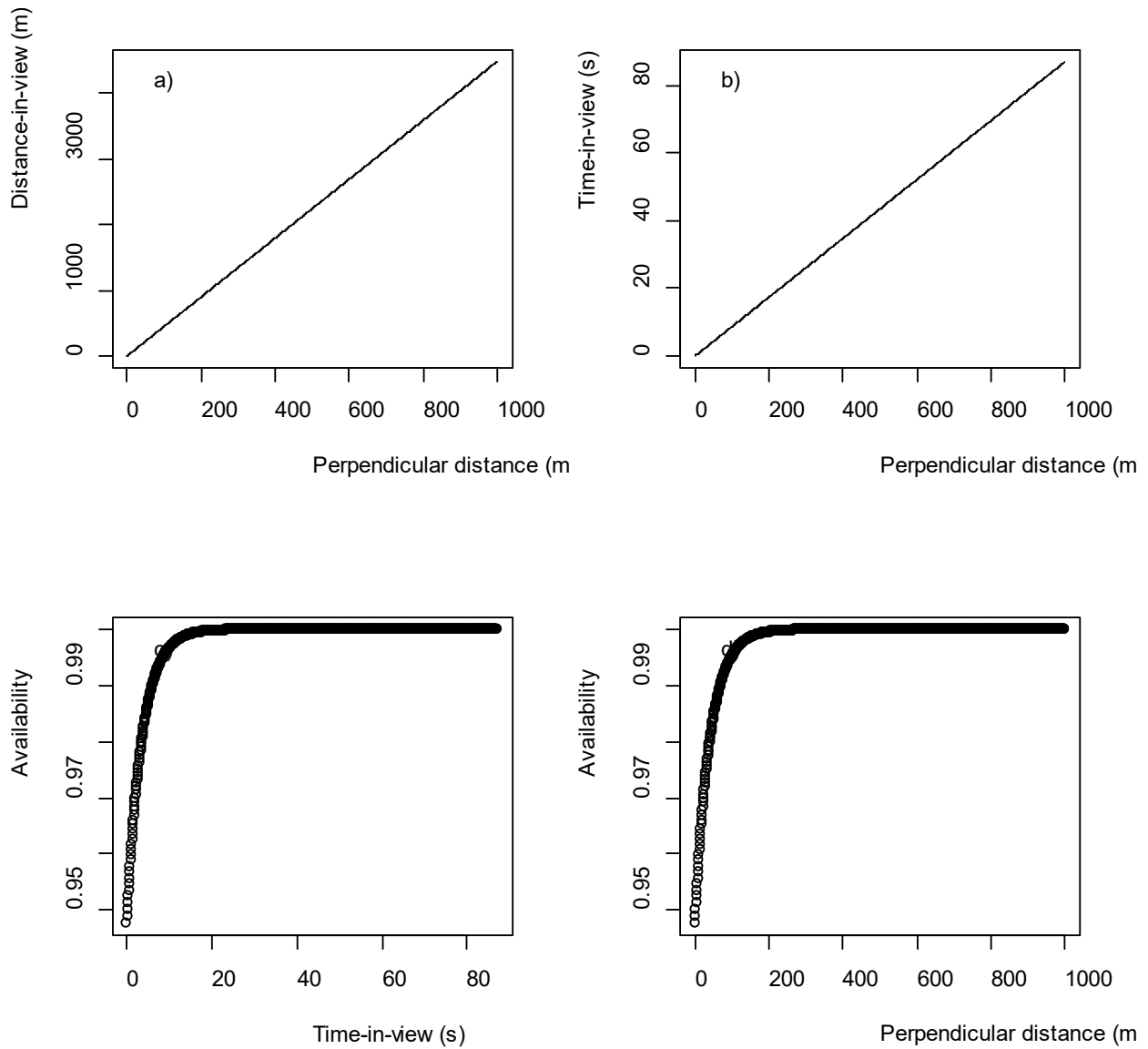


Figure A2. Simulated change in a) distance-in-view with perpendicular distance; b) time-in-view with perpendicular distance; c) availability with time-in-view; and d) availability with perpendicular distance, assuming a mean dip duration of 3.6 s and mean surface interval of 67 s, as observed for belugas in zone 1 with a 2 m turbidity threshold.

APPENDIX 3. PROBABILITY OF A BELUGA BEING CAPTURED IN AT LEAST ONE OF TWO CONSECUTIVE PHOTOGRAPHS AS A FUNCTION OF TIME LAPSE BETWEEN FRAMES, ESTIMATED FROM TAG DATA

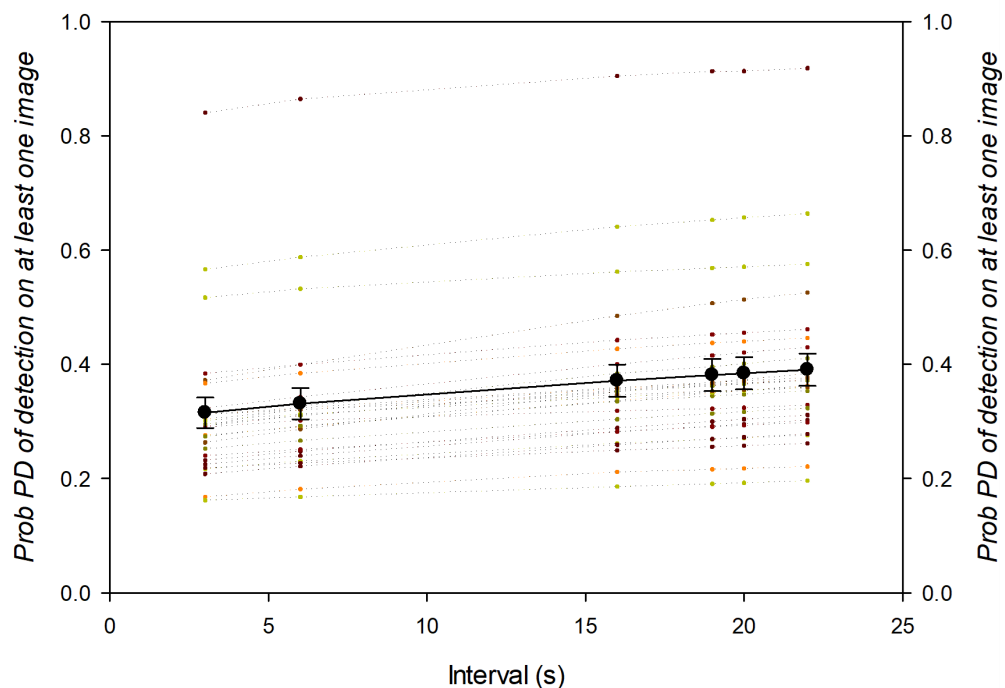


Figure A3. Mean (solid line) and individual (dotted lines) probability PD (and standard error) of being at the surface at least once in images taken at different time intervals, estimated using 27 beluga equipped with time-depth recorders. The average turbidity for the study area (i.e., 4 m) was used as the threshold for beluga capturability at the surface.

Table A3. Values corresponding to Figure A3.

Turbidity (m)	Empirical P_D given shutter time interval (s)					
	3	6	16	19	20	22
4	0.315 (0.027)	0.331 (0.027)	0.371 (0.028)	0.381 (0.028)	0.384 (0.028)	0.390 (0.028)

APPENDIX 4. MEAN DIVE, SURFACE TIMES AND AVAILABILITY FOR PHOTOGRAPHIC AND VISUAL SURVEYS

Table A4. Weighted average (and weighted standard error) of a) surface intervals (s), and dive durations (d) when using 0.5 m to define a dive, and either all 27 individuals or only beluga that have used each of the three zones (Zone 1, 2 and 3) identified in the St. Lawrence Estuary; and of b) availability P [i.e., $s / (s + d)$] when using different thresholds to define a dive and considering each time all 27 individuals (All zones). Zone 1 corresponds to the Upper Estuary; zone 2 is the southern portion of the Lower Estuary; and zone 3 is the northern portion of the Lower Estuary (see Figure 2). Availability is uncorrected for photo overlap or shutter speed (i.e., P and not \bar{P})*

Table 4a. Using 0.5 m to define a dive.

Turbidity zone	N	Mean s (in s)	Mean d (in s)
All Zones	27	51.6 (4.5)	176.6 (12.6)
Zone 1	9	41.2 (7.6)	174.1 (30.1)
Zone 2	8	41.2 (2.3)	180.6 (10.3)
Zone 3	21	60.1 (5.3)	176.8 (12.8)

Table 4b. Using different thresholds to define a dive.

Threshold (m)	N	Mean availability Photographic ¹	Mean availability Visual ²
0.5	27	0.063 (0.003)	0.233 (0.012)
2	27	0.272 (0.012)	0.319 (0.014)
4	27	0.367 (0.019)	0.378 (0.020)
5	27	0.398 (0.020)	0.403 (0.020)
8	27	0.440 (0.018)	0.440 (0.018)

¹ If dip time below turbidity threshold is included as part as dive time

² If dip time below turbidity threshold is included as part of surface time

APPENDIX 5. DIVE TIME (D): ESTIMATED REGRESSION PARAMETERS FOR A GAMMA GAMM APPLIED TO D .

Dive threshold = 0.5 m

Table A5.1 Model selection. Optimal model (bold) based on lowest AIC.

	<i>df</i>	AIC
<i>M0.ed : Intercept only</i>	25.7	19507.4
<i>M1.ed : Zone</i>	27.8	19505.7
<i>M2.ed : Depth + Zone</i>	35.3	19466.7
<i>M3.ed : Depth</i>	33.1	19470.8
<i>M4.ed : AHD</i>	26.7	19506.9
<i>M5.ed : Zone + AHD</i>	28.8	19504.3
<i>M6.ed : Depth + Zone + AHD</i>	36.2	19463.3
<i>M7.ed : depth + AHD</i>	34.0	19468.3

Table A5.2. Parameters for the optimal model. The estimated value for σ_{a_i} is 0.384.

	Estimate	Std. error	<i>t</i> or <i>F</i> value	<i>P</i> -value
Intercept	5.34661	0.09932	53.834	< 0.0001
Zone 5 m	-0.21642	0.09435	-2.294	0.0219
Zone 8 m	-0.17748	0.08059	-2.202	0.0278
Outside AHD	-0.11352	0.04781	-2.375	0.0177
s(Seafloor depth) ^a			8.294	< 0.0001

^a *edf* = 7.069

The fitted model is as follows:

$$d_{ij} \sim \text{Gamma}(\mu_{ij}, r)$$

$$d_{ij}] = \mu_{ij}$$

$$\text{var}[d_{ij}] = \mu_{ij}^2 / 2.12$$

$$\mu_{ij} = \exp(5.346 + f(\text{Depth}) + a_i) \quad \text{for Zone} = 2 \text{ m and AHD} = \text{in}$$

$$\mu_{ij} = \exp(5.346 - 0.216 + f(\text{Depth}) + a_i) \quad \text{for Zone} = 5 \text{ m and AHD} = \text{in}$$

$$\mu_{ij} = \exp(5.346 - 0.177 + f(\text{Depth}) + a_i) \quad \text{for Zone} = 8 \text{ m and AHD} = \text{in}$$

$$\mu_{ij} = \exp(5.346 - 0.113 + f(\text{Depth}) + a_i) \quad \text{for Zone} = 2 \text{ m and AHD} = \text{out}$$

$$\mu_{ij} = \exp(5.346 - 0.216 - 0.113 + f(\text{Depth}) + a_i) \quad \text{for Zone} = 5 \text{ m and AHD} = \text{out}$$

$$\mu_{ij} = \exp(5.346 - 0.177 - 0.113 + f(\text{Depth}) + a_i) \quad \text{for Zone} = 8 \text{ m and AHD} = \text{out}$$

Dive threshold = 4 m

Table A5.3 Model selection. Optimal model (bold) based on lowest AIC.

	df	AIC
M0.ed : Intercept only	26.8	19807.2
M1.ed : Zone	28.8	19804.5
M2.ed : Depth + Zone	36.7	19739.8
M3.ed : Depth	34.6	19744.9
M4.ed : AHD	27.7	19807.7
M5.ed : Zone + AHD	29.8	19804.2
M6.ed : Depth + Zone + AHD	37.7	19738.4
M7.ed : depth + AHD	35.5	19744.7

Table A5.4 Results for the optimal model applied to beluga dive time (d). The estimated value for σ_{a_i} is 0.575.

	Estimate	Std. error	t or F value	P-value
Intercept	5.19533	0.13793	37.667	< 0.0001
Zone 5 m	-0.30515	0.11618	-2.627	0.0087
Zone 8 m	-0.22061	0.10119	-2.180	0.0294
Outside AHD	-0.11045	0.05736	-1.926	0.0543
s(Seafloor depth) ^a			12.84	< 0.0001

^a edf = 7.921

The fitted model is as follows:

$$d_{ij} \sim \text{Gamma}(\mu_{ij}, r)$$

$$E[d_{ij}] = \mu_{ij}$$

$$\text{var}[d_{ij}] = \mu_{ij}^2 / 1.544$$

$$\mu_{ij} = \exp(5.1953 + f(\text{Depth}) + a_i)$$

for Zone 1 = 2 m and AHD = in

$$\mu_{ij} = \exp(5.1953 - 0.305 + f(\text{Depth}) + a_i)$$

for Zone 2 = 5 m and AHD = in

$$\mu_{ij} = \exp(5.1953 - 0.221 + f(\text{Depth}) + a_i)$$

for Zone 3 = 8 m and AHD = in

$$\mu_{ij} = \exp(5.1953 - 0.11045 + f(\text{Depth}) + a_i)$$

for Zone 1 = 2 m and AHD = out

$$\mu_{ij} = \exp(5.1953 - 0.11045 - 0.305 + f(\text{Depth}) + a_i)$$

for Zone 2 = 5 m and AHD = out

$$\mu_{ij} = \exp(5.1953 - 0.11045 - 0.221 + f(\text{Depth}) + a_i)$$

for Zone 3 = 8 m and AHD = out

Dive threshold = 2, 5 and 8 m for zone 1, 2 and 3, respectively

Table A5.5 Model selection. Optimal model (bold) based on lowest AIC.

	df	AIC
M0.ed : Intercept only	25.5	19698.9
M1.ed : Zone	28.8	19804.5
M2.ed : Depth + Zone	34.9	19607.8
M3.ed : Depth	33.2	19628.5
M4.ed : AHD	26.5	19695.7
M5.ed : Zone + AHD	28.6	19687.1
M6.ed : Depth + Zone + AHD	36.0	19602.0
M7.ed : depth + AHD	34.3	19621.2

Table A5.6. Results for the optimal model applied to beluga dive time [E(d)]. The estimated value for σ_{a_i} is 0.456.

	Estimate	Std. error	t or F value	P-value
Intercept	5.40073	0.11708	46.129	< 0.0001
Zone 5 m	-0.40426	0.11886	-3.401	0.0007
Zone 8 m	-0.55956	0.10173	-5.500	< 0.0001
Outside AHD	-0.17355	0.06045	-2.871	0.0041
s(Seafloor depth) ^a			17.35	< 0.0001

^a edf = 7.715

The fitted model is as follows:

$$d_{ij} \sim \text{Gamma}(\mu_{ij}, r)$$

$$E[d_{ij}] = \mu_{ij}$$

$$\text{var}[d_{ij}] = \mu_{ij}^2 / 1.315$$

$$\mu_{ij} = \exp(5.401 + f(\text{Depth}) + a_i)$$

for Zone 1 = 2 m and AHD = in

$$\mu_{ij} = \exp(5.401 - 0.404 + f(\text{Depth}) + a_i)$$

for Zone 2 = 5 m and AHD = in

$$\mu_{ij} = \exp(5.401 - 0.560 + f(\text{Depth}) + a_i)$$

for Zone 3 = 8 m and AHD = in

$$\mu_{ij} = \exp(5.401 - 0.174 + f(\text{Depth}) + a_i)$$

for Zone 1 = 2 m and AHD = out

$$\mu_{ij} = \exp(5.401 - 0.404 - 0.174 + f(\text{Depth}) + a_i)$$

for Zone 2 = 5 m and AHD = out

$$\mu_{ij} = \exp(5.401 - 0.560 - 0.174 + f(\text{Depth}) + a_i)$$

for Zone 3 = 8 m and AHD = out

APPENDIX 6. SURFACE TIME (S): ESTIMATED REGRESSION PARAMETERS FOR A GAMMA GAMM APPLIED TO S.

Dive threshold = 0.5 m

Table A6.1 Model selection. Optimal model (bold) based on lowest AIC.

	df	AIC
M0.es : Intercept only	25.1	15790.0
M1.es : Zone	26.8	15790.8
M2.es : Depth + Zone	33.1	15793.1
M3.es : Depth	30.5	15790.9
M4.es : AHD	26.1	15790.5
M5.es : Zone + AHD	27.8	15791.9
M6.es : Depth + Zone + AHD	34.0	15794.9
M7.es : depth + AHD	31.5	15792.5

Table A6.2. Parameters for the optimal model. The estimated value for σ_{a_i} is 0.496.

	Estimate	Std. error	t or F value	P-value
Intercept	3.8949	0.1088	35.78	<0.0001

The fitted model is as follows:

$$s_{ij} \sim \text{Gamma}(\mu_{ij}, r)$$

$$E[s_{ij}] = \mu_{ij}$$

$$\text{var}[s_{ij}] = \mu_{ij}^2 / 0.835$$

$$\mu_{ij} = \exp(3.895 + a_i)$$

Dive threshold = 4 m

Table A6.3 Model selection. Optimal model (bold) based on lowest AIC.

	df	AIC
M0.es : Intercept only	24.9	17707.7
M1.es : Zone	26.6	17710.7
M2.es : Depth + Zone	29.8	17716.3
M3.es : Depth	28.2	17713.6
M4.es : AHD	25.9	17709.3
M5.es : Zone + AHD	27.6	17712.0
M6.es : Depth + Zone + AHD	30.9	17718.1
M7.es : depth + AHD	29.2	17715.3

Table A6.4 Parameters for the optimal model. The estimated value for σ_{a_i} is 0.379.

	Estimate	Std. error	t or F value	P-value
Intercept	4.31704	0.08957	48.2	<0.0001

The fitted model is as follows:

$$s_{ij} \sim \text{Gamma}(\mu_{ij}, r)$$

$$E[s_{ij}] = \mu_{ij}$$

$$\text{var}[s_{ij}] = \mu_{ij}^2 / 1.175$$

$$\mu_{ij} = \exp(4.317 + a_i)$$

Dive threshold = 2, 5 and 8 m for zone 1, 2 and 3, respectively

Table A6.5 Model selection. Optimal model (bold) based on lowest AIC. Models within $\Delta\text{AIC} = 5$ may be pure noise. Two models make ΔAIC range to 7 (intercept-only and AHD only). However, Depth is not significant, and Zone effect is only based on difference in estimated s between 2 m and 8 m.

	df	AIC
<i>M0.es : Intercept only</i>	24.9	17793.9
<i>M1.es : Zone</i>	25.8	17789.3
M2.es : Depth + Zone	30.4	17788.3
<i>M3.es : Depth</i>	29.4	17789.9
<i>M4.es : AHD</i>	25.9	17795.7
<i>M5.es : Zone + AHD</i>	26.8	17791.2
<i>M6.es : Depth + Zone + AHD</i>	31.4	17790.1
<i>M7.es : depth + AHD</i>	30.4	17791.9

Table A6.6 Parameters for the intercept-only model. The estimated value for σ_{a_i} is 0.374.

	Estimate	Std. error	t or F value	P-value
Intercept	4.2930	0.1091	39.36	<0.0001

^a $edf = 22.72$

The fitted model is as follows:

$$s_{ij} \sim \text{Gamma}(\mu_{ij}, 0.7744)$$

$$E[s_{ij}] = \mu_{ij}$$

$$\text{var}[s_{ij}] = \mu_{ij}^2 / 0.7744$$

$$\mu_{ij} = \exp(4.2930 + a_i)$$

APPENDIX 7. PROPORTION OF TIME AT SURFACE (P): ESTIMATED REGRESSION PARAMETERS FOR A BETA GAMM APPLIED TO P

Dive threshold = 4 m

Table A7.1 Model selection. Optimal model (bold) based on lowest AIC.

	<i>df</i>	AIC
<i>M0.photo : Intercept only</i>	24.5	-717.3
<i>M1.photo: Zone</i>	26.4	-714.6
<i>M2.photo: Depth + Zone</i>	31.6	-736.6
<i>M3.photo: Depth</i>	29.7	-739.1
<i>M4.photo: AHD</i>	25.4	-715.5
<i>M5.photo: Zone + AHD</i>	27.3	-713.1
<i>M6.photo: Depth + Zone + AHD</i>	32.4	-735.2
<i>M7.photo: depth + AHD</i>	30.6	-737.5

Table A7.2 Parameters for the optimal model. The estimated value for σ_{a_i} is 0.318.

	Estimate	Std. error	<i>t</i> or <i>Chi.sq</i> value	<i>P</i> -value
Intercept	-0.52668	0.06856	-7.682	<0.0001
s(Seafloor depth) ^a			38.99	<0.0001

^a *edf* = 5.981

The fitted model is as follows:

#' $P_{ij} \sim \text{beta}(P_{ij}, \theta = 4.049)$

#' $E[P] = P_{ij}$

#' $\text{logit}(P_{ij}) = \exp(-0.52668 + f(\text{Depth}) + a_i)$

Dive threshold = 2, 5 and 8 m for zone 1, 2 and 3, respectively

Table A7.3 Model selection. Optimal model (bold) based on lowest AIC.

	<i>df</i>	AIC
<i>M0.photo : Intercept only</i>	24.4	-567.1
<i>M1.photo: Zone</i>	24.3	-615.8
<i>M2.photo: Depth + Zone</i>	25.0	-618.7
<i>M3.photo: Depth</i>	30.6	-577.0
<i>M4.photo: AHD</i>	25.4	-574.6
<i>M5.photo: Zone + AHD</i>	25.5	-620.8
<i>M6.photo: Depth + Zone + AHD</i>	26.0	-624.1
<i>M7.photo: depth + AHD</i>	26.4	-573.3

Table A7.4 Parameters for the optimal model. The estimated value for σ_{a_i} is 0.297.

	Estimate	Std. error	z or Chi-sq	P-value
Intercept	-1.14801	0.10345	-11.097	< 0.0001
Zone 5 m	0.58540	0.11599	5.047	< 0.0001
Zone 8 m	0.82996	0.09903	8.381	< 0.0001
Outside AHD	0.17099	0.06395	2.674	0.0075
s(Seafloor depth) ^a			6.657	< 0.0001

^a edf = 1.000

The fitted model is as follows:

$P_{ij} \sim \text{beta}(P_{ij}, \theta = 3.38815)$

$E[P_{ij}] = P_{ij}$

$\text{logit}(P_{ij}) = \exp(-1.14801 + f(\text{Depth}) + a_i)$ for 2 m and AHD = in

$\text{logit}(P_{ij}) = \exp(-1.14801 + 0.585 + f(\text{Depth}) + a_i)$ for 5 m and AHD = in

$\text{logit}(P_{ij}) = \exp(-1.14801 + 0.830 + f(\text{Depth}) + a_i)$ for 8 m and AHD = in

#

$\text{logit}(P_{ij}) = \exp(-1.14801 + 0.171 + f(\text{Depth}) + a_i)$ for 2 m and AHD = out

$\text{logit}(P_{ij}) = \exp(-1.14801 + 0.171 + 0.585 + f(\text{Depth}) + a_i)$ for 5 m and AHD = out

$\text{logit}(P_{ij}) = \exp(-1.14801 + 0.171 + 0.830 + f(\text{Depth}) + a_i)$ for 8 m and AHD = out

APPENDIX 8. DEVIANCE EXPLAINED BY THE DIFFERENT MODELS

Table A8. Deviance explained by models best fitting the data for dive time d , surface time s , and instantaneous availability P . Threshold (in m) represents the minimum depth for defining a dive (d and s), or the mean or zone-specific turbidity threshold for defining the proportion of time beluga are available for detection during photographic surveys (P).

Threshold (m)	d	s	P
0.5 m	21.8%	14.3%	-
4 m	28.9%	15.1%	21.3%
2, 5, 8 m	22.6%	17.8%	26.4%